

SELF-SIMILAR SOLUTIONS OF TWO-DIMENSIONAL CONSERVATION LAWS

Barbara Lee Keyfitz *

ABSTRACT. Self-similar reduction of an important class of two-dimensional conservation laws leads to boundary value problems for equations which change type. We have established a method for solving free boundary problems for quasilinear degenerate elliptic equations which arise when shocks interact with the subsonic (nonhyperbolic) part of the solution. This paper summarizes the principal features of the method.

A preliminary version of these notes formed the basis of a series of three lectures at the Newton Institute in April, 2003. They are a report of research carried out jointly with Sunčica Čanić, Eun Heui Kim and Gary Lieberman.

CONTENTS

| | | |
|----------|--|-----------|
| 1 | Introduction | 2 |
| 2 | Two-Dimensional Conservation Laws with Acoustic Structure | 3 |
| 3 | Quasi-One-Dimensional Riemann Problems: Hyperbolic Region | 9 |
| 4 | Quasilinear Degenerate Elliptic Equations of Keldysh Type | 13 |
| 4.1 | Linear and Nonlinear Behavior at the Sonic Line | 19 |
| 4.2 | Transport Equations and Vorticity | 20 |
| 5 | A Catalog of Free Boundary Problems | 21 |
| 5.1 | Hyperbolic Free Boundary Problems | 22 |
| 6 | A Fixed Point Approach to the Existence of Transonic Shocks | 25 |
| 7 | Existence of a Subsonic Solution: the Uniformly Elliptic Case | 34 |
| 7.1 | L^∞ Bounds and Monotonicity | 35 |
| 7.2 | The Fixed Point of the Mapping | 38 |
| 8 | The Degenerate Elliptic Free Boundary Problem | 42 |
| 8.1 | Local Lower Barriers and Convergence | 42 |
| 8.2 | Verification of the Solution | 43 |
| 8.3 | Convergence at the Degenerate Boundary | 43 |

*Department of Mathematics, University of Houston, Houston, Texas 77204-3008. Research supported by the National Science Foundation, Grant DMS 03-06307 and the Department of Energy, Grant DE-FG02-03ER25575.

| | |
|--|-----------|
| 9 The Solution of the Self-Similar System | 44 |
| 10 Acknowledgements | 46 |
| 11 REFERENCES | 46 |

1 INTRODUCTION

Little has been proved about systems of conservation laws in more than two variables. About ten years ago, Sunčica Čanić, David Wagner and I [15] began to analyse some simple problems by assuming symmetry, or self-similarity, in the solutions and reducing systems in two space variables and time to systems in two variables. This approach has the potential to demonstrate what sorts of singularities may occur in solutions. Interesting problems in two-dimensional conservation laws which are naturally self-similar include the von Neumann paradox of regular and irregular reflection.

We began by analysing the *unsteady transonic small disturbance (UTSD) equation*, Example 4.4, following work of Brio and Hunter [2] and of Tabak and Rosales [47] which developed this equation as an asymptotic reduction of the compressible gas dynamics equations in the case of weak shocks and small deviation from one-dimensional flow. (In particular, the system (4.4) described in Example 4.4 is irrotational and the spatial symmetry has been broken). Morawetz [43] has shown how this system arises in the reflection of a shock by a wedge.

Earlier work of Zhang and Zheng [49] had already provided a framework for self-similar reduction of the gas dynamics equations; Serre [45] has found that some a priori estimates for the reduced equations. An important point made in this pioneering research is that the self-similar system changes type; our contribution was to recognize that the equations which characterize the subsonic flow exhibit a novel type of elliptic degeneracy, and to begin an analysis of it. The first result was an existence theorem by Choi, Lazer and McKenna [23] for a quasilinear degenerate elliptic equation, motivated by the problem we consider here. Čanić and I first showed the existence of weak solutions (in Sobolev spaces) to the elliptic equation arising in the UTSD system [3, 5], and showed how this might apply to self-similar problems for the UTSD equation [4, 8]. We then began developing the general framework we report on here [6, 7]. At the same time, Zheng and co-workers began a similar program, which also involves free boundary problems for a degenerate elliptic equation closely related to ours, [35, 46, 50, 51, 52]. Shuxing Chen and co-workers are championing a different approach to free boundary problems arising in shock perturbation, using a partial hodograph transformation, see for example [20, 21].

There is a tension between the goals of developing a general theory and gaining experience by solving prototype problems. We have chosen the latter course. In suggesting broader motivation, we recognize that two-dimensional Riemann

problems may not play the same key role in multidimensional conservation laws that the one-dimensional Riemann problem has served for problems in a single space variable. One-dimensional Riemann problems give both the short-time, local behavior and the asymptotic global behavior of one dimensional systems; they are the building blocks of powerful existence theorems; they are the basis of certain computational methods, in both one and several space dimensions; and they provide a set of benchmark problems for evaluating the accuracy of numerically computed solutions. Except for the last, multidimensional Riemann problems are not expected to do any of those things. (One can imagine a two-dimensional Glimm scheme based on rectangles or hexagons, or possibly on a nonstructured grid which uses the most important wave directions, but it is not at all clear how to make this work.) Indeed, while one-dimensional Riemann problems simply express the way the standard diagonalization of a one-dimensional hyperbolic system via characteristic coordinates and characteristic speeds can be adapted to quasilinear systems, solving two-dimensional problems involves the much less transparent character of two-dimensional nonlinear wave propagation. One of our goals is to analyse this: to show that solutions of certain kinds exist, and to develop a criterion for deciding between different solutions when the self-similar solution is not unique. This is not the same as determining whether numerical simulations match experiments, although definitive analytical results may be helpful there, too. The numerical literature is too rich to survey here, but we mention recent work of Alexander Kurganov and co-workers [37], which underlies the simulations reproduced in Figures 5.2 and 7.3.

The salient fact about the self-similar problems discussed in these notes is that they lead to free boundary problems for quasilinear elliptic equations with novel types of degeneracies. Working with Gary Lieberman, we developed an approach to these problems, initially applied to a steady transonic equation [14]. Lieberman's theory of oblique derivative boundary value problems in Lipschitz domains forms the technical infrastructure for our approach. After Eun Heui Kim, who had studied degenerate elliptic equations with Choi [22, 33] joined our group as a postdoctoral visitor, we carried out the analysis for some weak shock reflection configurations for the UTSD equation [9, 10, 12]. Most recently, we have realized that self-similar reduction of the gas dynamics equations leads to systems which are of mixed type, not merely degenerate elliptic, in the subsonic region [11], and we have completed our first analysis of such a case [13]. This paper gives an outline of our approach and examples of our results.

2 TWO-DIMENSIONAL CONSERVATION LAWS WITH ACOUSTIC STRUCTURE

A system of conservation laws in two space variables and time,

$$U_t + F(U)_x + G(U)_y = 0, \quad U, F, G \in \mathbb{R}^n, \quad (2.1)$$

has the quasilinear form

$$P(\partial, U)U \equiv (\partial_t + A(U)\partial_x + B(U)\partial_y)U = 0.$$

Solutions which are functions of the variables $\xi = x/t$ and $\eta = y/t$ satisfy the reduced equation

$$-\xi U_\xi - \eta U_\eta + F(U)_\xi + G(U)_\eta = 0,$$

which can be written in conservation form ($\Xi = (\xi, \eta)$):

$$\tilde{F}(U, \Xi)_\xi + \tilde{G}(U, \Xi)_\eta \equiv (F(U) - \xi U)_\xi + (G(U) - \eta U)_\eta = -2U,$$

or as a quasilinear system

$$\tilde{P}(\partial, \Xi, U)U \equiv \tilde{A}U_\xi + \tilde{B}U_\eta \equiv (A(U) - \xi)U_\xi + (B(U) - \eta)U_\eta = 0. \quad (2.2)$$

Here $A = dF$ and $B = dG$ are the Jacobian matrices of F and G .

The sort of Cauchy problem for (2.1) which gives rise to self-similar solutions is data of the form

$$U(x, y, 0) = U^0(\theta), \quad \text{where } x = r \cos \theta, \quad y = r \sin \theta,$$

since the scaling $U(x, y, t) \mapsto U(\lambda x, \lambda y, \lambda t)$ leaves the solution invariant. Thus, in principle, a ‘two-dimensional Riemann problem’ is any Cauchy problem for (2.1) in which the initial data are constant on rays through the origin¹. However, our approach requires that the solution be known at a finite distance from the origin, and hence we typically consider sectorially constant data: U^0 takes constant values in a finite number of wedges, separated by lines of discontinuity, as in Figure 3.1. We have found a complete solution to this problem in only a single case, so far, and only for a simple problem with two distinct constant values [13]. Nonetheless, it is useful to think about more general problems that might be treated this way. In particular, with shock reflection problems in mind, we do not restrict consideration to problems where the data are constant in orthogonal quadrants; nor do we focus only on those where each sector boundary propagates as a single wave. Work of Zhang and Zheng [49], and others [17], has classified data with these two properties for the gas dynamics equations.

Before examining the Riemann problem for (2.1), we recall that the characteristics in a system like (2.1) differ both from characteristics in one space dimension and from characteristics in a scalar multidimensional equation. In either of those contexts, characteristics can be described by ordinary differential equations, and the nature of wave propagation in the equation is ‘along the characteristics’. (Strictly speaking, signals propagate along bicharacteristic strips; however, characteristic surfaces are easily identified with bicharacteristics for a single equation or in the case of two independent variables.)

¹I am indebted to Martin Kruskal for this observation.

For a linear first-order system in \mathbb{R}^d , with principal part

$$P(\partial, \mathbf{x}) = \sum_1^d A_i(\mathbf{x})\partial_{x_i}$$

acting on a state variable $U \in \mathbb{R}^n$, a *characteristic surface* is defined by means of its *characteristic normal*, ν , in a dual space \mathbb{R}_d , which satisfies

$$p(\nu, \mathbf{x}) \equiv \det P(\nu, \mathbf{x}) = \det \left(\sum_1^d A_i(\mathbf{x})\nu^i \right) = 0. \quad (2.3)$$

The operator is said to be *hyperbolic* if (2.3) has a maximal set of real roots and corresponding null vectors. To make this precise, fix a normal direction $\nu_0 \in \mathbb{R}_d$; then ν_0 is a *timelike normal* and the operator P is *hyperbolic* with respect to that normal if $p(\nu_0, \mathbf{x}) \neq 0$, if the roots $\lambda(\nu)$ of

$$p(\lambda\nu_0 + \nu, \mathbf{x}) = 0$$

are real, and if the null vectors form a basis for \mathbb{R}^n for all $\nu \notin \text{span}\{\nu_0\}$.

For each $\mathbf{x} \in \mathbb{R}^d$, the set of characteristic normals forms a cone, the *characteristic cone* or *normal cone*, $\mathcal{C}_N(\mathbf{x})$, which lies in the dual space, \mathbb{R}_d . Characteristic hyperplanes are subsets of physical space, \mathbb{R}^d , whose tangent plane at \mathbf{x} is normal to a vector in $\mathcal{C}_N(\mathbf{x})$. At \mathbf{x} , the equation $PU = 0$ expresses a constraint on the function U restricted to the characteristic surface. Specifically, suppose that a function $U^0(\mathbf{x})$ is given on a surface in a neighborhood of a point \mathbf{x}_0 , and hence that all tangential derivatives of U^0 along the surface at \mathbf{x}_0 are known. Then the equation $P(\partial, \mathbf{x})U = 0$ can be solved to determine the derivative of U normal to the surface, $\partial_\nu U$, precisely when $p(\nu, \mathbf{x}) \neq 0$. This idea dates back to the Cauchy-Kowalevski theorem, and the definition above applies also to a quasilinear equation, in which the matrices A_i depend on U ; the direction of the characteristic normals then depends on the value of U^0 at \mathbf{x} . The definition is local unless the A_i are constant. A *characteristic surface* is a surface in \mathbb{R}^d whose normal is characteristic at every point.

The dimension associated with a characteristic surface is $d-1$. It is convenient to define a particular, singular characteristic surface, the *wave cone* at \mathbf{x} , by taking the envelope of all the characteristic hyperplanes through a point \mathbf{x} . For a hyperbolic operator, this surface bounds the domain of influence of data at the point \mathbf{x} .

The general definition given above is useful when we look at self-similar reductions like (2.2), but for the most part one deals with equations in which the time variable has been specified, (my convention is to make it the n^{th} coordinate, consistent with the usual way axes are pictured), and hyperbolicity is measured with respect to the normal $(0, 0, \dots, 1)$. When applied to a system in a single space variable,

$$U_t + F(U)_x \equiv U_t + A(U)U_x = 0,$$

this means that $\nu_0 = (0, 1)$ and we can take $\nu = (-1, 0)$ without loss of generality. Then we have the familiar condition $\det(\lambda I - A(U)) = 0$ for the ‘characteristics’, λ . However, strictly speaking, ‘characteristics’ are vectors, $(-1, \lambda)$, in a space of characteristic normals (which is seldom invoked in one-dimensional problems), and the corresponding ‘characteristic surfaces’, now curves, in physical space, are curves with normal $(-1, \lambda)$ or tangent $(\lambda, 1)$ in (x, t) -space; that is, the integral curves of

$$\frac{dx}{dt} = \lambda(U(x, t)).$$

The D’Alembert solution for the wave equation expresses the way the solution ‘propagates along characteristics’ in one space dimension, and also shows that the domain of dependence includes the entire interior of the wave cone.

A single equation in \mathbb{R}^d is always hyperbolic; any variable whose coefficient A_i in P is nonzero is timelike. Now the differential operator itself is a directional derivative, $P = \mathbf{A} \cdot \nabla$, along a characteristic surface, which is therefore foliated by *bicharacteristic curves*: the integral curves of this operator. But if we are dealing with systems of first-order equations or with second-order equations like the wave equation, this is no longer the case: although the influence of information at a point is confined to the domain of dependence, which is the convex hull of the wave cone, it is not accurate to say that solutions ‘propagate along characteristics’.

In general, the characteristic structure for a hyperbolic system may be quite complicated. The point of departure for our analysis is an observation about the characteristics of the compressible gas dynamics equations in two or three space dimensions. In three space dimensions, the quasilinear Eulerian system for isentropic gas dynamics is

$$\begin{aligned} \rho_t + (\rho u)_x + (\rho v)_y + (\rho w)_z &= 0 \\ (\rho u)_t + (\rho u^2 + p)_x + (\rho uv)_y + (\rho uw)_z &= 0 \\ (\rho v)_t + (\rho uv)_x + (\rho v^2 + p)_y + (\rho vw)_z &= 0 \\ (\rho w)_t + (\rho uw)_x + (\rho vw)_y + (\rho w^2 + p)_z &= 0. \end{aligned} \tag{2.4}$$

Writing (2.4) in the quasilinear form $U_t + \sum A_i(U)U_{x_i} = 0$, where U may be the vector of conserved quantities or any other convenient set of state variables (since this does not affect the hyperbolic structure), taking t as the timelike direction and introducing the dual vector (μ, τ) , one finds that

$$p = \lambda^2(\lambda^2 - c^2|\mu|^2),$$

where $\lambda = \tau + \mu \cdot \mathbf{u}$ and $\mathbf{u} = (u, v, w) \in \mathbb{R}^3$ is the velocity vector. That is, the system is hyperbolic with respect to t , and the characteristic polynomial p can be factored into two linear factors and one nondegenerate quadratic one. The quadratic factor generates the acoustic wave cone which typifies the behavior of this system, as well as that of the linear wave equation. This structure is not the

only one which can arise in physical problems: in the equations of magnetohydrodynamics, \mathcal{C}_N contains several separate nondegenerate cones, while in other systems, such as zero-pressure gas dynamics, p is a product of linear factors. However, a certain structure, which we term ‘acoustic’, seems to characterize many important systems, such as compressible gas dynamics. It is defined as follows, where we now specialize to two space dimensions.

DEFINITION 2.1 ([7], ASSUMPTION 1) *A quasilinear hyperbolic system*

$$P(\partial, U)U = U_t + AU_x + BU_y = 0,$$

for $U \in \mathbb{R}^n$, is of acoustic type if the characteristic determinant factors into linear and quadratic parts,

$$\det P(\sigma, U) = \left(\prod_1^{n-2} \ell_i \cdot \sigma \right) q(\sigma, U),$$

where $\sigma = (\mu, \nu, \tau)$ is the dual vector to (x, y, t) , and q is a quadratic form.

If q is quadratic and the system is hyperbolic, then one can further write $q(\sigma, U) = \sigma^T Q_N(U) \sigma$, where Q_N is a 3×3 symmetric matrix with eigenvalues $\lambda_1, \lambda_2 > 0 > \lambda_3$. The nondegenerate part of the normal cone is

$$\mathcal{C}_V(U) = \{\sigma \mid \sigma^T Q_N(U) \sigma = 0\}$$

and its dual, the nondegenerate wave cone, is

$$\mathcal{C}_W(U) = \{\mathbf{x} \mid \mathbf{x}^T Q_W(U) \mathbf{x} = 0\}$$

with $Q_W = Q_N^{-1}$. It is convenient to assume, in addition, that the degenerate normal directions, the planes $\ell_i \cdot \sigma = 0$, lie outside \mathcal{C}_V . In this case, the directions inside \mathcal{C}_V are *timelike normals* and their duals in \mathbb{R}^3 are *spacelike planes*. Systems of acoustic type behave predictably under the self-similar reduction introduced at the beginning of this section.

PROPOSITION 2.2 ([7], THEOREM 2.1) *For a quasi-linear system in two space variables and time, at any fixed state U , the reduced system (2.2) is hyperbolic at precisely the points $\Xi = (\xi, \eta)$ such that $\mathbf{x} = (\xi, \eta, 1)$ is outside the conic \mathcal{C}_W . The nondegenerate characteristics at a hyperbolic point Ξ are tangent to the conic.*

DEFINITION 2.3 ([7]) *The sonic line or sonic circle $\mathcal{B}_U \in \mathbb{R}^2$ is the locus of points where the reduced equation changes type from hyperbolic to nonhyperbolic. This curve is the conic section*

$$\mathcal{B}_U = \mathcal{C}_W \cap \{t = 1\} = \{(\xi, \eta) \mid (\xi, \eta, 1) Q_W(\xi, \eta, 1)^T = 0\}.$$

Its interior is the subsonic region.

If the original operator is hyperbolic with respect to the time variable, then \mathcal{B}_U is a circle or an ellipse. For the reduced system, hyperbolicity depends both on Ξ and on U .

DEFINITION 2.4 ([7]) *Define $(\Xi, U) \in \mathbb{R}^2 \times \mathbb{R}^n$ to be a hyperbolic pair if the operator $\tilde{P}(\partial, \Xi, U)$ is hyperbolic.*

Change of type occurs in a neighborhood of the set

$$\mathcal{B} \equiv \{(\Xi, U) \mid (\xi, \eta, 1)Q_W(U)(\xi, \eta, 1)^T = 0\} \subset \mathbb{R}^2 \times \mathbb{R}^n.$$

The sonic line is the projection of \mathcal{B} into physical space; we introduce the term *sonic locus* for its projection into state space. The shape of the sonic locus is determined by the nonlinear structure of the flux functions.

Steady ‘transonic’ equations, obtained from (2.1) by looking for solutions independent of t , can also be considered as a type of reduced system; in this case $\tilde{A} = A$, $\tilde{B} = B$ and the position of sonic points is independent of Ξ . The term ‘quasi-steady’ is often used to refer to the self-similar flows discussed in this paper, and some analogies with steady transonic flow are helpful. However, in developing a mathematical theory, the fact that the quasi-steady equations are hyperbolic far from the origin in all directions is a great simplification over steady transonic flow, and suggests that well-posed problems can be formulated for (2.2).

EXAMPLE 2.5 It is instructive to apply this approach to the linear wave equation, $u_{tt} = c^2 \Delta u$, in two space dimensions. This was done by Keller and Blank [31]. With any sectorially constant self-similar data, the one-dimensional solutions (plane waves viewed in the self-similar physical plane) propagate on lines tangent to the sonic circle $\xi^2 + \eta^2 = c^2$, interacting with each other by linear superposition to produce new, ever piecewise constant, states; the characteristic lines do not change. The complete solution in the hyperbolic region terminates at the sonic line with a set of data consisting of a finite number of piecewise constant states on the sonic circle. The linear degenerate elliptic equation with these data, which must be solved inside the circle, was transformed by Keller and Blank to Laplace’s equation by a ‘Busemann transform’. They found that the solution displayed a square-root singularity as it approached the parts of the boundary where the data were constant. At discontinuities, the solution was smoothed out in the interior of the circle, but approached every intermediate value as the boundary was approached from different directions.

This example illustrates some of the features of quasilinear self-similar problems: wave interactions in the hyperbolic region and degenerate elliptic equations in the subsonic region. The missing ingredient, which we find in quasilinear problems, is the necessity of solving free boundary problems for the position of the sonic line and for transonic shocks, coupled with the subsonic flow.

3 QUASI-ONE-DIMENSIONAL RIEMANN PROBLEMS: HYPERBOLIC REGION

We now regard (2.2) as the basic equation, and replace the sectorially constant Riemann data, with which we suppose it to have been furnished, by the collection of one-dimensional Riemann solutions at infinity. It should be clear that $t \rightarrow 0$ corresponds to $\xi^2 + \eta^2 \rightarrow \infty$ for all $(x, y) \neq (0, 0)$. For states U_L and U_R separated by a discontinuity on the line $x = \kappa y$, one-dimensional Riemann problems are of the form

$$U(x, y, 0) = \begin{cases} U_L, & x < \kappa y \\ U_R, & x > \kappa y \end{cases} . \quad (3.1)$$

Their solutions are (self-similar) functions of $x - \kappa y$ and t ; $U = V(x - \kappa y, t)$, and $V(z, t)$ is a solution depending on z/t of the one-dimensional system $V_t + (F(V) - \kappa G(V))_z = 0$. Let us suppose that all the one-dimensional Riemann problems corresponding to the discontinuities of the initial data can be solved (for example, we could assume data of small oscillation, although that is not in the spirit of this work). In particular, admissibility conditions must typically be imposed on the shocks that arise; again, assume this has been done.

Our notation is awkward in some respects: in the one-dimensional problems (3.1), horizontal lines correspond to $\kappa = \infty$, the terms ‘left’ and ‘right’ do not make sense and the solution formulas are slightly different from classical one-dimensional theory. We made this choice rather than use a more cumbersome notation throughout.

With respect to data given at a large distance from the origin, the forward wave cone of \tilde{P} at a hyperbolic point $\Xi \in \mathbb{R}^2$ is bounded by the extreme characteristics directed towards the origin. (Lines through Ξ that do not intersect the cone are spacelike.) Thus, the one-dimensional Riemann solutions may be regarded as waves propagating inward from infinity. Naively, one might suppose that they define the solution until the intersection of local solutions coming from one-dimensional waves with different slopes. However, this may not always be the case. Locally, at a point Ξ , one has a concept of domain of determinacy given by the extreme characteristics corresponding to the solution U at Ξ ; however, Ξ is also downstream from (that is, in the domain of influence of) a half-space worth of data. Since there is no maximum principle for the system, there is no a priori bound on how far from the origin Ξ must be to guarantee that the one-dimensional solution described above is found there. For specific problems, this difficulty can be handled; we await further experience before formulating any general principles.

Adopting the naive point of view, we visualize the existence of a circle $\xi^2 + \eta^2 = C^2$ which is large enough that the known one-dimensional solutions are valid there. We may now think of these solutions as giving rise to Cauchy data (and relatively straightforward Cauchy data, consisting of constant states, shocks, rarefaction waves and linear discontinuities) on the circle, and, again a bit naively, one might visualize solving the problem in the forward time-like direction using

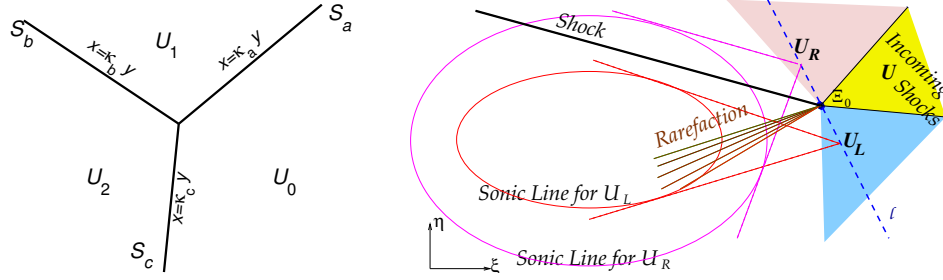


FIGURE 3.1: Sectorial Data and Quasi-One-Dimensional Riemann Problems

the hyperbolicity of the problem to construct the solution locally. The intersection of lines of discontinuity gives rise to what we have termed ‘quasi-one-dimensional Riemann problems’, see Figure 3.1.

DEFINITION 3.1 ([7], DEFINITION 4.1) *A quasi-one-dimensional Riemann problem for the self-similar equation $\tilde{P}U = 0$ consists of the data triple (Ξ_0, U_L, U_R) given on a line ℓ through Ξ_0 which is spacelike with respect to both states. The subscripts refer to left and right of an observer at Ξ_0 facing toward forward time.*

Although the system (2.2) is not of conventional one-dimensional form (since the fluxes depend on Ξ), quasi-one-dimensional Riemann problems admit solutions with the same structure as classical one-dimensional Riemann problems — that is, solutions consisting of a sequence of n shocks, rarefaction waves centered at Ξ_0 , and linear waves, with angles decreasing as one goes clockwise from U_L , separated by constant states. The discontinuities are simply planar shocks and linear waves which pass through Ξ_0 . Admissibility conditions for shocks can be formulated as in any one-dimensional problem, and are the standard admissibility conditions for one-dimensional systems $V_t + (F - \kappa G)_z = 0$. Rarefactions are solutions of the form $U = V((\xi - \xi_0)/(\eta - \eta_0))$. This structure follows from

PROPOSITION 3.2 ([7], PROPOSITION 3.1) *Let $U = V(h(\xi, \eta))$ be a simple wave solution of $\tilde{P}U = 0$. Then V' is an eigenvector of $\tilde{P}((h_\xi, h_\eta), \Xi, U)$ and the corresponding characteristic family forms straight lines.*

Thus, a quasi-one-dimensional Riemann solution looks just like a one-dimensional solution, suitably translated and rotated. Quasi-one-dimensional Riemann problems do not always have solutions, and the solutions are not necessarily unique. First, it is clearly necessary that the pairs (Ξ, U_L) and (Ξ, U_R) both be hyperbolic, in order for the curve ℓ to be spacelike. In addition, the loci of points in state space that can be connected to a state U_0 by an admissible quasi-one-dimensional shock through the point Ξ_0 may not be curves extending to infinity but instead may form a loop, like the shock polar of steady flow, [7]. See Figure 3.2. We have not tried to formulate an existence theory for these problems, except locally near the sonic line [7].

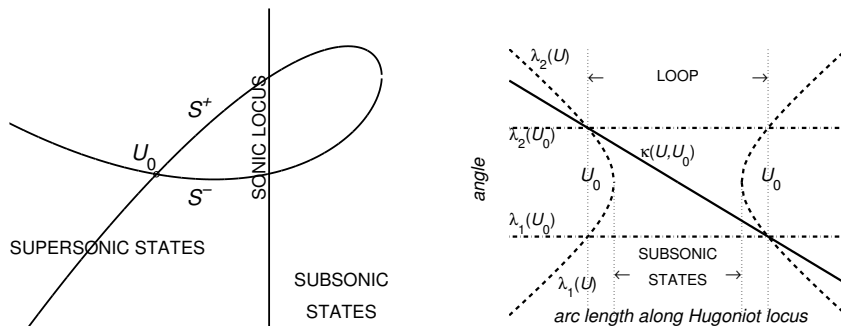


FIGURE 3.2: The Shock Polar and Variation of the Shock Angle

Following local Riemann solutions in the forward timelike direction is what is done in front-tracking, and, as in front-tracking, the intersection of rarefaction waves is more complicated to track since the interaction is not localized at a point in physical space and it does not result in piecewise constant solutions nor in centered rarefactions. As in one-dimensional problems, we expect the interactions to result in outgoing waves of about the same strength and composition as the incoming waves, with some perturbations added. We have not tackled this question, but note that the key thing to prove is the existence of outgoing perturbed rarefactions up to the points where the solution becomes sonic. Since a rarefaction is composed of straight line characteristics, by Proposition 3.2, each ray in a rarefaction is tangent to a sonic line; after the ray has touched the sonic line, it can be continued, but this would correspond to moving backward in time and is not a valid solution. Figure 3.3 shows a typical configuration when a centered rarefaction ends at a sonic line.

We now look more closely at shock admissibility conditions for the acoustic waves. In the case of the gas dynamics equations, the extreme characteristics are the nondegenerate characteristics corresponding to the acoustic speeds. Furthermore, these characteristics are also genuinely nonlinear in the sense of nonlinear conservation laws. We recall the definitions:

DEFINITION 3.3 *A characteristic speed $\tau(\mu, \nu, U)$ of $P(\partial, U)U = 0$ is genuinely nonlinear in the direction of a characteristic normal σ if*

$$R_\sigma \cdot \nabla_U \tau \neq 0$$

for a characteristic vector R_σ with $P(\sigma, U)R_\sigma = 0$.

The concept of genuine nonlinearity in higher dimensions generalizes and extends the one-dimensional notion. When restricted to plane waves — one-dimensional waves in higher dimensions — this reduces to the one-dimensional definition, and means that nonconstant waves are either compression or rarefaction waves. At a point in physical space, the normal direction of the wave, σ , may determine

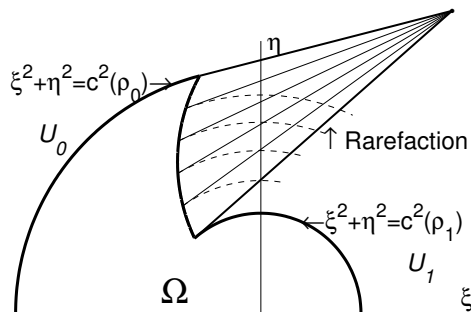


FIGURE 3.3: A Simple Wave Ending at the Sonic Line

whether it is genuinely nonlinear or not, and in which directions it is a compression. The acoustic waves in the gas dynamics equations (always a useful point of reference) are uniformly genuinely nonlinear in all directions as a consequence of the equivariance of the system under Euclidean coordinate changes, while the other characteristic families are not only degenerate in the sense of contributing linear factors to the characteristic polynomial but are also linearly degenerate in the classical, conservation laws sense.

In devising prototype systems to study, it is useful to keep these properties in mind. We recall in passing the well-known fact that a scalar conservation law in two or more space dimensions cannot be genuinely nonlinear in every direction. Furthermore, at least in two-dimensional systems which respect Euclidean symmetries, the possibility of genuinely nonlinear characteristic fields seems to be connected to the existence of both invariant and equivariant components of U . Three equations and a characteristic structure including one co-existing linear family seems to be the smallest size for a system with acoustic behavior which models compressible gas dynamics [32]. This has motivated our study of the nonlinear wave system, Example 4.6, as a prototype.

If one assumes that the acoustic waves form the extreme characteristics, and that they are genuinely nonlinear, then it can be shown that for pairs (Ξ_0, U_0) that are close to sonic, the curve of states that can be connected to U_0 via an admissible shock passing through the point Ξ_0 is indeed a loop, the shock polar, [7, Theorem 3.1]. As U traverses the loop, the shock angle κ varies from the larger to the smaller of the two acoustic characteristic angles of $U_0(\Xi_0)$; we might use the terms ‘-’ and ‘+’ or ‘left’ and ‘right’ to designate the two families of shocks (the terms ‘slow’ and ‘fast’ do not seem appropriate). Figure 3.2 gives a sketch of a typical shock polar in phase space and shows how the angle κ varies along the shock polar.

Another way of viewing a quasi-one-dimensional shock is to compare a uniform, straight-line shock between two states U_0 and U_1 in (ξ, η) -space with the corresponding planar shock in (x, y, t) -space. As a consequence of genuine non-

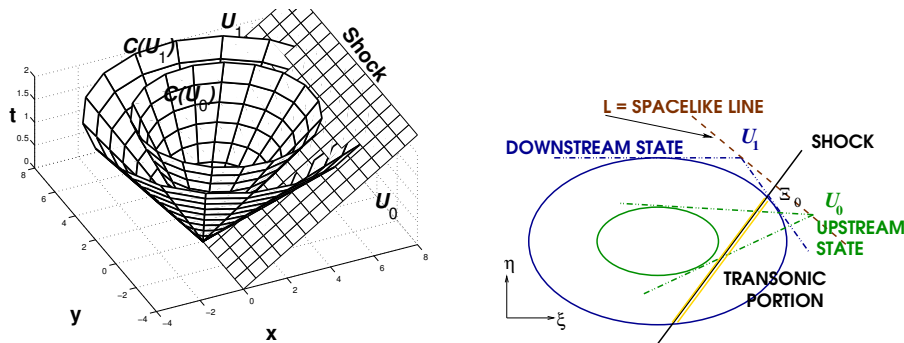


FIGURE 3.4: A Uniform Planar Shock and its Self-Similar Projection

linearity, in (x, y, t) -space the planar shock intersects the broader acoustic cone, but not the smaller one, as in the first picture in Figure 3.4. Thus, the shock surface is spacelike with respect to one of the two states. If the shock is admissible, then that state is ‘upstream’: for points near the shock on that side, every ray in the forward wave cone crosses the shock surface. (This means that the state influences the shock position, but no information about the shock influences the state.) When the same planar shock is viewed as a straight line shock in (ξ, η) -space, as in the second picture in Figure 3.4, the sonic curves of the two states are two circles or ellipses, and the shock intersects one and not the other. Since the smaller sonic circle lies across the shock from its corresponding state, that state is supersonic in the entire half-plane, while on the other side of the shock, the flow is subsonic inside the sonic line. Where the shock is supersonic, one can verify that the Lax geometric admissibility condition holds; the shock is a ‘plus’ or ‘right’ shock at one end and a ‘minus’ or ‘left’ shock when viewed from the other. In the transonic portion, the shock is supersonic with respect to the upstream state, just as in steady flow. The shock is normal somewhere in the middle of the transonic portion, and might be called a ‘left’ or ‘right’ shock on either side, but it is not clear that these terms make sense for a transonic shock.

In the same way, as one traverses in phase space the shock polar of a pair (Ξ_0, U_0) , the polar will cross the sonic locus twice, as the configuration goes from a ‘left’ to a transonic to a ‘right’ shock, as in the first picture of Figure 3.2.

4 QUASILINEAR DEGENERATE ELLIPTIC EQUATIONS OF KELDYSH TYPE

Before looking at the transition between super- and subsonic states, we examine the system in the subsonic region. When the equations are linearized about a constant state, we find degenerate elliptic equations of a particular type.

PROPOSITION 4.1 ([7], PROPOSITION 5.1) *If $n \geq 2$, the operator \tilde{P} , linearized at a constant state, can be written as a second-order operator which changes type, coupled through lower-order terms to a first-order hyperbolic system of order $n-2$.*

The form of the second-order equation near the sonic line is

$$x\phi_{xx} + \phi_{yy} + g(x, y, \nabla\phi, \psi) = 0. \quad (4.1)$$

Here the variables $(\nabla\phi, \psi)$, $\psi \in \mathbb{R}^{n-2}$ can be obtained from U by a linear coordinate change, and (x, y) is a coordinate system such that the sonic line is $\{x = 0\}$.

We note that only for linear systems might we expect to be able to decouple the elliptic subsystem from the rest of the problem; for nonlinear systems novel types of mixed problems may occur. Motivated by shock reflection problems, we are particularly interested in the case that U is constant along the degenerate boundary, as this situation arises when U is constant outside the sonic line. It is useful to be able to write a second-order equation for one variable, to represent the ‘elliptic’ part of the system. Some examples suggest the range of situations which can occur.

EXAMPLE 4.2 Isentropic compressible gas dynamics. A second-order equation in similarity variables (ξ, η) can be written for the density, ρ . The original system is

$$\begin{aligned} \rho_t + (\rho u)_x + (\rho v)_y &= 0 \\ (\rho u)_t + (\rho u^2 + p)_x + (\rho uv)_y &= 0 \\ (\rho v)_t + (\rho uv)_x + (\rho v^2 + p)_y &= 0; \end{aligned} \quad (4.2)$$

The self-similar equations, ignoring conservation form, are

$$\begin{aligned} (u - \xi)\rho_\xi + \rho u_\xi + (v - \eta)\rho_\eta + \rho v_\eta &= U\rho_\xi + \rho u_\xi + V\rho_\eta + \rho v_\eta = 0 \\ (u - \xi)u_\xi + p_\xi/\rho + (v - \eta)u_\eta &= Uu_\xi + p_\xi/\rho + Vu_\eta = 0 \\ (u - \xi)v_\xi + (v - \eta)v_\eta + p_\eta/\rho &= Uv_\xi + Vv_\eta + p_\eta/\rho = 0; \end{aligned}$$

$U = u - \xi$, $V = v - \eta$ are the components of the ‘pseudovelocity’. We see that, unlike steady transonic flow, Example 4.5, and like the nonlinear wave system, Example 4.6, the distinction between supersonic and subsonic regions depends on position in space as well as on the states. A version that refers only to the pseudovelocity is [11, 45]

$$\begin{aligned} U\rho_\xi + \rho U_\xi + V\rho_\eta + \rho V_\eta + 2\rho &= 0 \\ UU_\xi + p_\xi/\rho + VU_\eta + U &= 0 \\ UV_\xi + VV_\eta + p_\eta/\rho + V &= 0. \end{aligned}$$

The second-order equation for ρ is

$$\begin{aligned} \partial_\xi((U^2 - c^2)\rho_\xi + UV\rho_\eta) + \partial_\eta((V^2 - c^2)\rho_\eta + UV\rho_\xi) + (\rho U)_\xi + (\rho V)_\eta \\ + (UV_\eta - VU_\eta)\rho_\xi + (VU_\xi - UV_\xi)\rho_\eta + 2(U_\xi V_\eta - V_\xi U_\eta)\rho = 0. \end{aligned} \quad (4.3)$$

The sonic line is the circle $U^2 + V^2 = c^2(\rho)$ in (ξ, η) -space. A framework for solving this system is to regard (4.3) in the subsonic region as an equation for ρ whose coefficients evolve according to transport equations along pseudo-streamlines:

$$\begin{aligned}(U, V) \cdot \nabla u &= -p_\xi / \rho \\ (U, V) \cdot \nabla v &= -p_\eta / \rho.\end{aligned}$$

There is an analogy with the simpler nonlinear wave system, described below, but we have not yet extended our method to the gas dynamics equation.

EXAMPLE 4.3 The adiabatic Euler equations can be put in a form like this, with a second-order equation for the pressure, coupled now with three evolution equations for u , v and the density along streamlines, [11, 45].

EXAMPLE 4.4 The unsteady transonic small disturbance (UTSD) equation is used to model the transition between regular and irregular reflection for weak shocks [2, 29]. It takes the form

$$\begin{aligned}u_t + uu_x + v_y &= 0 \\ v_x - u_y &= 0,\end{aligned}\tag{4.4}$$

and yields the reduced system

$$\begin{aligned}(u - \xi)u_\xi - \eta u_\eta + v_\eta &= 0 \\ v_\xi - u_\eta &= 0.\end{aligned}\tag{4.5}$$

This system has only two equations, and no linear waves; in the subsonic region the self-similar equation is elliptic. A disadvantage is that t , which does not represent time but instead distance along rays, is not a timelike variable. Although this equation has a nondegenerate wave cone structure, the characteristic normal cone contains the direction $(0, 0, 1)$ as a generator, and the (x, y) -plane is a characteristic surface. A second-order equation for u in self-similar variables is

$$\left((u - \xi)u_\xi - \eta u_\eta \right)_\xi + u_{\eta\eta} = 0.\tag{4.6}$$

Alternatively, introducing a velocity potential ϕ , with $\nabla\phi = (u, v)$, one obtains

$$\phi_{xt} + \phi_x \phi_{xx} + \phi_{yy} = 0.$$

The sonic line for this system is the parabola $\xi + \eta^2/4 = u$; replacing ξ in (4.6) with the variable $\rho = \xi + \eta^2/4$ results in a system with diagonal principal part:

$$\left((u - \rho)u_\rho + \frac{u}{2} \right)_\rho + u_{\eta\eta} = 0.\tag{4.7}$$

The noncompactness of the sonic line for the linearized system is a consequence of the fact that the (x, y) -plane in the space-time system is characteristic. For either the space-time system (4.4) or its self-similar reduction, a complete characterization of well-posed problems is still an open problem.

EXAMPLE 4.5 The full potential equation of transonic gas dynamics. The original system is [43]

$$\begin{aligned}\rho_t + \nabla \cdot (\rho \nabla \Phi) &= 0 \\ \Phi_t + \frac{1}{2} |\nabla \Phi|^2 + i(\rho) &= \text{const}\end{aligned}$$

for density ρ and a velocity potential Φ . Introducing similarity variables and the reduced potential, with $\Phi = t\phi(\xi, \eta)$, $\varphi = \phi - \frac{1}{2}(\xi^2 + \eta^2)$, yields

$$\begin{aligned}\nabla \cdot (\rho \nabla \varphi) + 2\rho &= 0 \\ \frac{1}{2} |\nabla \varphi|^2 + \varphi + \frac{c^2(\rho)}{\gamma - 1} &= \text{const.}\end{aligned}\tag{4.8}$$

The second equation is solved for ρ and this solution is then used in the first. The result is again a second order equation which changes type when $|\nabla \varphi|^2 = c^2(\rho)$. Our method does not work on this problem, since the coefficients in the second-order operator in (4.8) depend on the gradient of the variable φ as well as on φ itself. Chen and Feldman [18, 19], using a different fixed point procedure, have solved free boundary problems connected with shock perturbation for this equation.

EXAMPLE 4.6 The nonlinear wave system (NLWS). This system is obtained either from the isentropic gas dynamics system by neglecting terms which are quadratic in the velocity, or by writing the nonlinear wave equation as a first-order system. In terms of the conserved quantities (density and momenta) the system is

$$\begin{aligned}\rho_t + m_x + n_y &= 0 \\ m_t + p_x &= 0 \\ n_t + p_y &= 0;\end{aligned}\tag{4.9}$$

here $p = p(\rho)$ represents pressure, with $p' = c^2(\rho)$, and $(m, n) = (u\rho, v\rho)$ is the momentum vector.

The system in self-similar coordinates reads

$$\begin{aligned}-\xi\rho_\xi - \eta\rho_\eta + m_\xi + n_\eta &= 0 \\ -\xi m_\xi - \eta m_\eta + p_\xi &= 0 \\ -\xi n_\xi - \eta n_\eta + p_\eta &= 0.\end{aligned}\tag{4.10}$$

The density satisfies a second-order equation:

$$\rho_{tt} = -(m_x + n_y)_t = -(m_t)_x - (n_t)_y = p_{xx} + p_{yy} = \nabla \cdot (c^2(\rho)\nabla \rho).$$

In self-similar coordinates, we have

$$((c^2 - \xi^2)\rho_\xi - \xi\eta\rho_\eta)_\xi + ((c^2 - \eta^2)\rho_\eta - \xi\eta\rho_\xi)_\eta + \xi\rho_\xi + \eta\rho_\eta = 0. \quad (4.11)$$

The important simplification over Example 4.2 is the decoupling of the nonlinear variable ρ from the other components of the state variable.

EXAMPLE 4.7 The pressure-gradient system has been studied by Yuxi Zheng and others [46, 50]. This system can be derived from the adiabatic gas dynamics equations, and has the form

$$\begin{aligned} u_t + p_x &= 0 \\ v_t + p_y &= 0 \\ E_t + (up)_x + (vp)_y &= 0; \end{aligned} \quad (4.12)$$

with $E = \frac{1}{2}(u^2 + v^2) + p$. There is a close mathematical correspondence with the NLWS, as the nonlinear variable p in this system is exactly $c^2(\rho)$ in NLWS, if the gas law in Example 4.6 is taken to be $p(\rho) = e^\rho$. Equation (4.11), when written in terms of $c^2(\rho) = p$, becomes Zheng's governing equation

$$(p - \xi^2)p_{\xi\xi} - 2\xi\eta p_{\xi\eta} + (p - \eta^2)p_{\eta\eta} + \frac{1}{p}(\xi p_\xi + \eta p_\eta)^2 - 2(\xi p_\xi + \eta p_\eta) = 0. \quad (4.13)$$

Zheng proved existence of solutions in domains with fixed, smooth, degenerate boundaries [50] and Song generalized the result to nonsmooth boundaries containing the origin [46]. The pressure-density relation in the pressure-gradient system is not the same as that in NLWS, so $p = 0$, the vacuum state, although degenerate, is physically admissible.

EXAMPLE 4.8 The linear wave equation $f_{tt} = c^2\Delta f$ can be written as a system in several ways: if either $(u, v, w) = (f_t, -c^2f_x, -c^2f_y)$ or $(u, v_x, w_y) = (f, f_t, f_t)$ the system

$$\begin{aligned} u_t + v_x + w_y &= 0 \\ v_t + c^2u_x &= 0 \\ w_t + c^2u_y &= 0 \end{aligned} \quad (4.14)$$

results. It can also be written as a system of two equations,

$$\begin{pmatrix} u \\ v \end{pmatrix}_t = \begin{pmatrix} c & 0 \\ 0 & -c \end{pmatrix} \begin{pmatrix} u \\ v \end{pmatrix}_x + \begin{pmatrix} 0 & c \\ c & 0 \end{pmatrix} \begin{pmatrix} u \\ v \end{pmatrix}_y$$

by a change of variables which does not preserve the Euclidean symmetry and which does not extend to nonlinear equations. If we take $p = c^2\rho$ in (4.9), we obtain (4.14). However, self-similar data for Example 4.6 would satisfy a compatibility condition if they came from the second-order wave equation.

Following the derivation in Section 2, one can write the nondegenerate normal cone of the reduced problem as $\mathcal{C}_R(\vec{\alpha}; \Xi, U)$, where $\vec{\alpha} = (\alpha, \beta)$ is the vector dual to $(\xi, \eta) = \Xi$. From the characterization of the normal cone, we find $\mathcal{C}_R = \{\vec{\alpha} \mid \vec{\alpha}^T Q_R \vec{\alpha} = 0\}$, where

$$Q_R = \begin{pmatrix} -\xi & 1 & 0 \\ -\eta & 0 & 1 \end{pmatrix} Q_N(U) \begin{pmatrix} -\xi & -\eta \\ 1 & 0 \\ 0 & 1 \end{pmatrix}$$

can be derived from the original partial differential operator P . See [7] for more details. From Proposition 2.2 and Definition 2.3, the sonic line is characterized by $\det Q_R = 0$ and the nonhyperbolic states by $\det Q_R > 0$. As the examples in this section show, one can often obtain a second order equation for one variable (possibly coupled to other variables) which is elliptic in the subsonic region. We recall the following definition.

DEFINITION 4.9 *For a second order elliptic operator in two variables with principal part given by a matrix (a^{ij}) , with $a^{ij} = a^{ij}(\Xi, U)$, the ellipticity ratio $\lambda = \lambda(\Xi, U)$ is the ratio of the smaller to the larger eigenvalue of (a^{ij}) .*

The ellipticity ratio depends on the state U and on the position Ξ in similarity space, and can be computed by finding the eigenvalues of Q_R .

EXAMPLE 4.10 For the UTSD equation, (4.7), $\lambda = u - \rho = u - (\xi + \eta^2/4)$. In the NLWS, (4.11), or linear wave equation, Example 4.8, $\lambda = 1 - (\xi^2 + \eta^2)/c^2$.

Returning to (4.1), the linearization at a constant state, we note that its principal part has a degeneracy near $x = 0$ which is attached to the x derivatives of ϕ rather than to the y derivatives. This operator is different from the Tricomi operator, which is of the form $\phi_{xx} + x\phi_{yy}$. The difference has been known, since work of Kohn and Nirenberg [36] and Baouendi [1], to lead to loss of regularity in (4.1). Linear equations of the type (4.1) were studied by Keldysh [30], who showed that solutions are typically Hölder continuous but not differentiable at the degenerate boundary. When we first uncovered an equation of this form, ten years ago, in analysing the self-similar reduction of the UTSD equation, there was no literature on nonlinear versions of it. For a linear operator $L = a^{ij}\partial_i\partial_j + b^i\partial_i$, boundary conditions at a degenerate boundary with normal ν are governed by the Fichera function, (see [44] for background on this definition)

$$b \equiv (b^i - a_{x_j}^{ij})\nu_i.$$

Depending on the sign of b , boundary conditions may be assigned at the degenerate boundary, or that part of the boundary must be left without conditions. For equations in divergence form, the Fichera condition becomes a condition on coefficients of the first order derivative terms, and extending it to a nonlinear

equation seems impossible. Needless to say, in a nonlinear equation in which the condition for the boundary to be degenerate depends on the value of the solution there, one needs to be able to prescribe the solution at this part of the boundary. The existence theorems in [3, 5, 16] provide a partial resolution of this question.

4.1 LINEAR AND NONLINEAR BEHAVIOR AT THE SONIC LINE

Consider a boundary value problem for the quasilinear second-order equation arising in the UTSD system, (4.6), with part of the boundary degenerate and with u constant there. There exist weak solutions of two types: they may exhibit a square root singularity, or the solution may be Lipschitz up to the boundary, depending on what boundary conditions are prescribed on the regular parts of the boundary, [3, 5].

The linear wave equation, Example 4.8, is the linear model for the acoustic waves for all the systems studied here, and to the extent that vorticity waves do not play a dominant role (which is probably the case at the sonic line), its solutions at the sonic line are a guide. The self-similar solution of the linear wave equation is

$$u = a_1 \log \left(\frac{c + \sqrt{c^2 - r^2}}{r} \right) + a_2,$$

with $r = \sqrt{\xi^2 + \eta^2}$. This has a square-root singularity at $r = c$, the sonic line: the canonical linear behavior, in agreement with the fundamental solution of the wave equation in two space dimensions. (See also the discussion in Example 2.5.) For the nonlinear wave equation, $u_{tt} = \nabla \cdot (c^2(u) \nabla u)$, a calculation suggests that solutions of this form exist, but that there is also a solution which looks like

$$u = u_0 - \frac{c(u_0)}{p''(u_0)} (c(u_0) - r)$$

in the neighborhood of the sonic line $r = c(u_0)$. That is, near a sonic line where $u = u_0$ is constant (so the line is a segment of the circle $r = c(u_0)$), then we also expect to see a solution which is Lipschitz up to the boundary, with a fixed slope depending on the nonlinear pressure-density relation.

EXAMPLE 4.11 An example using the UTSD equation illustrates this dichotomy. The second order equation, (4.7), derived in Example 4.4, admits solutions depending on the single variable ρ , which can be found by integrating the equation. Since ρ measures distance from the sonic line, these solutions describe, to first order, the different kinds of qualitative behavior of solutions which are constant at the sonic line. Figure 4.1 illustrates the solutions. The sonic point has been chosen, without loss of generality, as $\rho = 0$. The subsonic solutions, with $u - \rho > 0$, comprise a one-parameter family of singular solutions, of the form $u = D\sqrt{-\rho}$, $D > 0$, and a one-parameter family of Lipschitz solutions, $u = \rho/(1 + \sqrt{1 - C\rho})$,

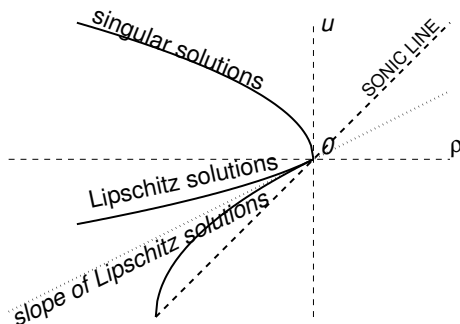


FIGURE 4.1: Singular and Regular Solutions, Example 4.11

all of which have slope $1/2$ at the origin. As the position of the arbitrary constant indicates, the first family is linear, the second nonlinear.

4.2 TRANSPORT EQUATIONS AND VORTICITY

Examples 4.2, 4.3, 4.4, 4.6 and 4.7 show that, in contrast to the linear problem analysed in Proposition 4.1, the reduction of nonlinear systems typically yields a second order equation for one variable (density or pressure) coupled to $n - 1$ transport equations from which the other variables can be recovered. For example, the second and third equations in (4.10) in Example 4.4 and the first and second equations in the self-similar version of (4.12) in Example 4.7, represent transport in the radial direction. In principle, using Proposition 4.1, we should integrate one of these equations and recover the other variable via a compatibility condition. In practice, it seems easier to integrate both and verify compatibility, as we do in Proposition 9.1 for the nonlinear wave system. There, whether the first component ρ is the singular or the Lipschitz solution of the NLWS near the sonic line, we calculate the functions m and n near $r = c(u_0)$ by integration.

By contrast, the UTSD equation illustrates the case $n = 2$ of Proposition 4.1. When $n = 2$, there are no transport equations. The variable v can be recovered by integrating the second equation of (4.4) (or its self-similar version), but this differs from the NLWS case. To detail the difference, we note that the theorems in [3, 5] determined only the first component, u , of solutions to the UTSD system, (4.6); the second component, v , is then determined by integrating one of the first-order equations in (4.5), and its boundary values on the degenerate boundary typically cannot be prescribed arbitrarily. This poses a difficulty when examining shock reflections modeled by this equation. Recall that, as illustrated in Example 4.11, there are singular and Lipschitz families of solutions u at the sonic line. When u is a member of the first family, it is not possible to find a solution for the second component v which approaches a constant value along the sonic line. (This can be done for the second family.) Hence weak reflected shocks, as in Example 6.1, do not exist for the UTSD system. Since neither the linear

wave equation (written as a system) nor the nonlinear wave system displays this paradoxical behavior, it is tempting to dismiss it as an anomaly of the UTSD system. However, this has not been resolved.

While we do not have proofs, we speculate that boundary behavior in the examples may be connected to vorticity in the self-similar problems we examine. Both the full potential equation and the UTSD equation assume an irrotational flow: $u_y = v_x$. By contrast, the full gas dynamics equations, either isentropic or adiabatic, make no such assumption. In fact, vorticity is generated in the solution by shocks, even if it is not present initially. The nonlinear wave system, which has been the focus of our recent research, is an uneasy compromise. Unlike the full potential or UTSD equations it does not contain an equation to enforce irrotationality. On the other hand, the quantity $w = m_y - n_x$ satisfies $w_t = 0$, and so the support of $m_y - n_x$, which is a sort of ‘specific vorticity’, is confined to its initial set. For weak shocks, vorticity, which is third order in shock strength, is not sufficient to resolve the triple point paradox, the gas dynamics analog of Example 5.3. In this respect, the NLWS and UTSD equations are of a kind, and model the von Neumann paradox.

The UTSD problems we solved in [3, 5] did not use boundary conditions taken from actual self-similar problems. Even in a simple example like the interaction of a rarefaction wave with the sonic line, as in Figure 3.3, there are portions of the sonic line where u is constant, and also portions where u is not constant. At least in examples such as Figure 3.3, the linearized equation is of Tricomi type at a sonic boundary where u is not constant. Furthermore, there is an interaction of the subsonic region with the hyperbolic region, which will typically change the location of the sonic line, as in Example 5.1. This remains an open problem.

We next examine the boundary value problems that arise at the sonic line.

5 A CATALOG OF FREE BOUNDARY PROBLEMS

We return to the quasi-one-dimensional front-tracking scenario of Section 3.

Eventually, as the solution is built up in the forward timelike direction, either as a limit of front-tracking approximations or directly by solving a finite number of quasi-one-dimensional Riemann problems exactly, one ends up at a sonic boundary. For the moment we omit consideration of cases where solving quasi-one-dimensional problems breaks down because a solution to the quasi-one-dimensional Riemann problem does not exist.

If we suppose that the subsonic region is connected, or examine a single component of it, then at points on the boundary three phenomena are possible:

1. The solution is continuous as the sonic line is approached, and U is constant on the hyperbolic side.
2. A shock of finite strength becomes transonic on one side and bends; the transonic shock becomes part of the boundary of the sonic region.

3. The solution is continuous up to the sonic line from both sides, but is not constant; rather, it consists of a simple wave (rarefaction) or a more complicated continuous hyperbolic solution.

In the first case, where the solution is constant on the hyperbolic side of the sonic line, then the acoustic characteristics become collinear there, and tangent to the boundary. The hyperbolic region is still upstream from the subsonic zone, even if only weakly so: we may assume that the solution is determined in the hyperbolic region (that is, the constant value determined from front-tracking is the solution), and proceed to seek a solution in the subsonic region.

In the second case, as stated earlier, the hyperbolic part of a transonic shock is strictly upstream from the shock: the nonlinear characteristics (and if we assume these are the extreme ones, the linear characteristics also) enter the shock from the hyperbolic side. Thus the flow is completely determined on the hyperbolic side. (In the unsteady cases we have considered up to now, it is also constant, but, as in steady transonic shock perturbation, [14], nonconstant hyperbolic flows can arise and could in principle be handled.) The shock is treated as a free boundary, which is coupled with the subsonic flow. In the problems we have solved, the subsonic flow can be found by solving a degenerate elliptic equation which is not coupled to the other variables. Other cases, such as the gas dynamics equations, in which the linear and nonlinear parts of the subsonic flow are strongly coupled, are ripe for attack.

The third type of behavior is more difficult to analyse than the first two. If a nonconstant hyperbolic solution (a rarefaction wave, for example) is extended to sonic points, then typically the characteristics become tangent to each other but not to the boundary. By looking at points in the hyperbolic region near the sonic line, one sees that the directions of forward time are opposite along the two parallel characteristics. That is to say, one characteristic flows into the subsonic region, and the other out of it. (The dashed curves in Figure 3.3 represent the characteristics flowing into the hyperbolic region.) In particular, the entire subsonic region influences every point reached by the ourward moving characteristics. In this case, it appears on the basis of careful numerical simulations that the extended hyperbolic solution is not actually the solution of the problem up to the sonic line. Instead, the sonic line itself becomes a free boundary, coupled both to the hyperbolic flow outside the subsonic region and to the mixed type equation inside. This leads to new types of hyperbolic free boundary problems, which we have not yet solved.

5.1 HYPERBOLIC FREE BOUNDARY PROBLEMS

We give two examples of how such problems may arise. The first is straightforward, and has been observed by Zheng and others, [51]. The second occurs in a prototype for Mach reflection and for the resolution of the ‘triple-point paradox’.

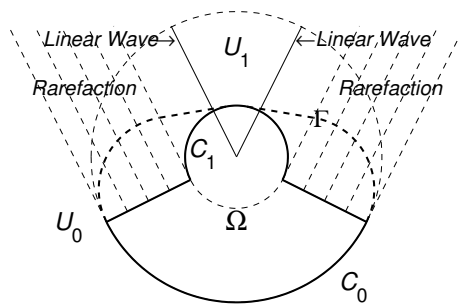


FIGURE 5.1: Rarefaction Waves in Example 5.1 and Domain of Determinacy

EXAMPLE 5.1 The equation is the nonlinear wave system, and the data consist of two states, U_1 above and U_0 below the lines $x = \pm\kappa y$, for $y \geq 0$. The states are chosen so that in the far field, each one-dimensional solution consists of a downward-moving rarefaction and a linear wave through the origin. Each straight-line characteristic in a rarefaction can persist until it reaches a sonic point; thus the rarefaction is defined on a half-strip, whose finite end is a straight line segment orthogonal to both the smaller (C_1) and larger (C_0) sonic circles. However, this sonic boundary is not a spacelike curve and so it is not in the domain of determinacy of the hyperbolic part of the problem. Instead, there is a curve Γ in the hyperbolic region which bounds the domain of determinacy of the supersonic flow. Within that curve, the flow no longer consists of rarefactions and constant states, and the sonic line (across which the solution may be continuous) is a free boundary. Furthermore, compression waves may form, and shocks may be generated; numerical calculations suggest that this is the case. See Figure 5.2, based on simulations by Alex Kurganov, where there appears to be a shock above the smaller sonic circle. Although this problem is still open, we mention that early work of Morawetz [42] on nonexistence of supersonic shock-free profiles suggests an approach to constructing continuous solutions if they exist.

EXAMPLE 5.2 In one case, the problem described in Example 5.1 has been solved. Dai and Zhang, [25], consider the self-similar equation arising from the pressure-gradient system, (4.13), with initial conditions corresponding to constant pressure $p > 0$ in one quadrant and vacuum in the other three. The solution has no subsonic region and no free boundary, as in this case the inner circle C_1 in Figure 5.1 shrinks to a point and the wedge in which $U = U_1$ (where $p = 0$) has opening angle $3\pi/2 > \pi$. The nonconstant region expands all the way to the Goursat boundary, Γ . The absence of a subsonic region occurs only in the case of a vacuum state. An interesting special feature of the self-similar pressure-gradient equation (4.13) contributed to the proof given by Dai and Zhang: The nonlinear equation, in polar coordinates, can be factored in an elegant way. The pressure-gradient equation, which we pointed out in Example 4.7 corresponds to an exponential gas law, is the only nonlinear wave equation with this property,

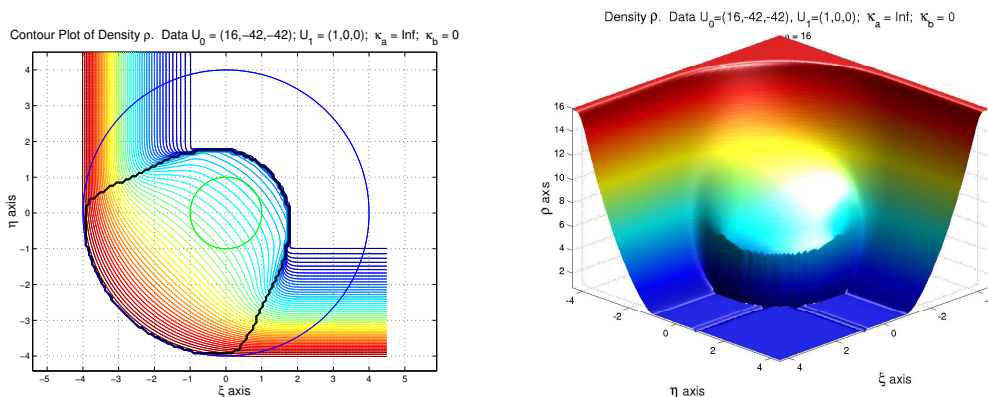


FIGURE 5.2: Contour Plot and Density Profile (Kurganov), Example 5.1

as was proved by Ferapontov and Khusnutdinova [26]. This property is related to integrability and to existence of Riemann invariants.

EXAMPLE 5.3 The free boundary problem described in Example 5.1 seems complicated. However, understanding it may help to explain one aspect of the ‘von Neumann paradox’: how a Mach stem with reflected wave can form in a system which does not permit triple points. A scenario can be given for the nonlinear wave system, as pictured in Figure 5.3; a similar picture can be drawn for the UTSD system. The picture involves a sonic state U_M interacting with the incident shock as a quasi-one-dimensional Riemann problem, resulting in a Mach stem (shock) and a small rarefaction wave. Our conjecture is that at a point Ξ_M outside the circle C_0 (which may or may not intersect the incident shock S_a^+), a sonic state U_M is formed; the quasi-one-dimensional Riemann problem for (U_1, U_M) at Ξ_M has a solution consisting of a shock (the Mach stem), intermediate supersonic state U_m and rarefaction (the curvilinear part of the shaded region in Figure 5.3). Between U_0 , the state across the incident shock from U_1 , and U_M is a reflected shock. Since U_M is exactly sonic, this shock must in fact bend immediately to become transonic. Thus it forms a free boundary (as does, separately, the Mach stem). The shaded region in Figure 5.3 is not a domain of determinacy, so its boundary is also free, as in Example 5.1. Note that U_0 is on the shock locus of U_1 and U_M on the shock locus of U_0 , at the sonic line; U_M is the intersection of the rarefaction locus through U_M and the shock locus of U_1 . We have $\rho_1 < \rho_0 < \rho_m < \rho_M$. There is a one-parameter family (parameterized by Ξ_M , with Ξ_M on S_a^+) of states satisfying these conditions. We conjecture that the location of Ξ_M depends on the remaining Riemann data. In this scenario, no linear waves appear (that is, no vorticity is generated), and a small hyperbolic patch is embedded in the subsonic region. The embedded hyperbolic patch is influenced by the subsonic flow, and hence the actual sonic line is contained somewhere within the region sketched here. Numerical evidence for

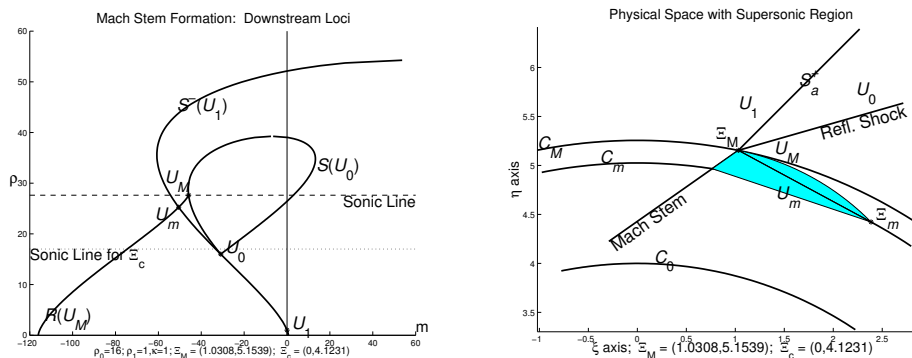


FIGURE 5.3: A Triple Point Construction, Example 5.3

a phenomenon like this in the UTSD equation has been obtained by Tesdall and Hunter [48].

6 A FIXED POINT APPROACH TO THE EXISTENCE OF TRANSONIC SHOCKS

We have devised an approach to solving free boundary problems of the type that arise in calculating the position of transonic shocks and the flow on the subsonic side. We have implemented this approach in several examples: perturbation of a steady shock in the steady transonic small disturbance equation; weak and strong regular reflection in the UTSD equation; and a type of Mach reflection in the NLWS in which the reflected wave is continuous (a compression wave). The following features characterise our approach:

1. The subsonic flow can be expressed via a second-order equation in a single variable (for example the density), in divergence form, which is quasilinear, degenerate elliptic, and whose coefficients depend on that variable, but not on its gradient. In particular, we do not use a velocity potential, even if one exists. The elliptic operator turns out to be uniformly elliptic on compact subsets of the subsonic region.
2. It is not necessary that the flow be irrotational. We note that allowing vorticity is important for projected application to the gas dynamics equations.
3. The conditions at the free boundary can be expressed as a pair of equations, one for the evolution of the boundary, which depends on the variable (but again not on its gradient) and one a quasilinear condition on the gradient of the variable, a so-called oblique derivative boundary condition. The oblique derivative operator must satisfy a uniform obliqueness condition, although we can handle some isolated degeneracies.
4. Standard boundary conditions (Dirichlet or Neumann) are applied on the fixed part of the boundary.

5. A priori conditions enable one to prove that the boundary is Lipschitz and piecewise $C^{1+\alpha}$, for some $\alpha > 0$, and that the corner angles are (approximately) known.
6. The free boundary can be written as a function with a fixed domain.

Before giving an outline of the method, we give as an example a problem we have successfully solved by this method.

EXAMPLE 6.1 The equation is the nonlinear wave system, and the Riemann data consist of two states, U_1 and U_0 , above and below the lines $x = \pm\kappa_a y$, for $y \geq 0$, with data chosen so that the one-dimensional Riemann problems in the far field are resolved by shocks moving upward and linear waves, which remain on the initial discontinuities. See Figure 6.1. In addition, κ_a is large enough that the incoming shocks become transonic before they intersect the symmetry axis (the η axis). (See Example 7.2 for a more complete analysis of the dependence of the solution of κ_a .) This is a prototype for Mach reflection by a wedge when the wedge angle is small. The second-order equation governing the subsonic flow is (4.11), which is of the form (6.5). Note, however, that we are using the nonlinear wave system, so that, although we expect similarities with the actual phenomena of weak shock reflection, we are not solving the gas dynamics equations. For sufficiently large κ_a (a bound comes from Lemma 8.5), a possible form of the solution is that the incoming shocks curve to form a Mach stem, and the flow is continuous everywhere else, but is not constant inside the sonic circle, the region Ω in Figure 6.1. We have proved that a solution of this form exists. In this case, the hyperbolic part of the solution contains four waves (two linear, two nonlinear) separated by constant states. The nonhyperbolic, subsonic part is the flow U inside the region bounded by the sonic circle of the state U_0 and the Mach stem, which is a free boundary, unknown a priori.

A simple example shows how to replace the standard Rankine-Hugoniot conditions at a shock by a derivative boundary condition for one of the variables and an evolution equation for the shock.

EXAMPLE 6.2 The *transonic small disturbance equation* is

$$\begin{aligned} uu_x + v_y &= 0 \\ v_x - u_y &= 0 \end{aligned} \tag{6.1}$$

This can be written as a second-order equation in u : $(uu_x)_x + u_{yy} = 0$, and so we want to convert the Rankine-Hugoniot conditions, which relate (u, v) in the subsonic region to a state (u_0, v_0) in the supersonic region on the other side of the shock, to conditions involving u and the shock angle alone. That is, with the shock angle given by $x = s(y)$, we want to eliminate v from the Rankine-Hugoniot equations

$$\frac{ds}{dy} = \frac{\frac{1}{2}(u^2 - u_0^2)}{v - v_0} = -\frac{v - v_0}{u - u_0}. \tag{6.2}$$

The linearity of the equations in v , which was a key to eliminating v from the system and obtaining a second-order equation, also allows us to solve for $v - v_0$ and obtain

$$\frac{ds}{dy} = \pm \sqrt{-\frac{u + u_0}{2}}. \quad (6.3)$$

The ambiguity in sign comes from the nonlinearity of the boundary condition, and some care, in the form of a priori bounds, must be taken to resolve it. In fact, it appears that losing single-valuedness of this solution corresponds to losing obliqueness of the derivative boundary condition. This may be not so much a limitation of the method as it is evidence that one needs additional conditions to get a well-posed problem. To treat the problem, we make one choice, say ‘-’, consistent with considering small perturbations of a ‘-’ shock.

To get a second boundary condition, which involves u and ∇u but not v , we solve the Rankine-Hugoniot equation (6.2) for v :

$$v = v_0 + (u - u_0) \sqrt{-\frac{u + u_0}{2}},$$

and differentiate this expression along Σ (letting $' = s' \partial_x + \partial_y = d/dy$ along Σ):

$$v' = v'_0 + (u' - u'_0) \sqrt{-\frac{u + u_0}{2}} - (u - u_0) \frac{(u' + u'_0)}{4 \sqrt{-\frac{u + u_0}{2}}}.$$

We express u' as $u_x s' + u_y$ and use the differential equation (6.1) to write

$$v' = v_x s' + v_y = u_y s' - u u_x;$$

substituting this for v' and collecting terms in u_x and u_y , we obtain

$$M u \equiv \beta^1(u; u_0, s') u_x + \beta^2(u; u_0, s') u_y = \chi(u; u_0, U'_0), \quad (6.4)$$

where

$$\begin{aligned} \beta^1(u; u_0, s') &= u + s' \left(\sqrt{-\frac{u + u_0}{2}} - \frac{u - u_0}{4 \sqrt{-\frac{u + u_0}{2}}} \right), \\ \beta^2(u; u_0, s') &= -s' + \sqrt{-\frac{u + u_0}{2}} - \frac{u - u_0}{4 \sqrt{-\frac{u + u_0}{2}}}, \\ \chi(u; u_0, U'_0) &= -v'_0 + u'_0 \left(\sqrt{-\frac{u + u_0}{2}} - \frac{u - u_0}{4 \sqrt{-\frac{u + u_0}{2}}} \right). \end{aligned}$$

(In some problems, we have found it advantageous to eliminate s' from (6.4) using (6.3).) Now (6.3) and (6.4) are the shock evolution equation and derivative boundary condition respectively.

Here is how we proceed in general. We wish to solve a quasilinear equation

$$Qu \equiv \partial_i(a^{ij}(u)\partial_j u) + b^i \partial_i u = 0 \quad (6.5)$$

in a region Ω which is not known a priori. The boundary of Ω has components of up to four types:

1. the free boundary, Σ , given by an equation $\eta(\xi)$, say, for $\xi \in [a, b]$; the function η satisfies

$$\frac{d\eta}{d\xi} = f(\xi, \eta, u), \quad (6.6)$$

for a Lipschitz function f , and an initial condition, $\eta(a) = \eta_0$, say, (thus, one end of the free boundary is known); in addition, on Σ u satisfies an oblique derivative boundary condition

$$Mu \equiv \beta \cdot \nabla u = \beta^i \partial_i u = g(\xi, \eta, u, \eta') \quad (6.7)$$

where the coefficients β^i are functions of ξ, η, u and η' and M is uniformly oblique;

2. the degenerate boundary, σ , on which the minimum eigenvalue of a^{ij} is zero, and on which u takes the constant value u_0 , say,

$$u|_{\sigma} = u_0; \quad (6.8)$$

3. the fixed nondegenerate boundary which may contain a component σ_0 on which Dirichlet data is given and a component Σ_0 on which Neumann data is given:

$$u|_{\sigma_0} = \phi, \quad \left. \frac{\partial u}{\partial \nu} \right|_{\Sigma_0} = \psi. \quad (6.9)$$

We assume that the boundary components meet at corners. One corner may not be known a priori — that corresponding to $\eta(b)$ — and hence one of the other curves is also not known completely. Rather than giving a formal definition which will include all cases, we assume that that curve can be extended. In fact, almost the first task is to impose a priori bounds on the function η which gives the position of the free boundary.

EXAMPLE 6.3 Let us see how this applies to Example 6.1 for the case of weak Mach reflection, with large κ_a . The degenerate boundary is the segment of the sonic circle which lies below the incident shocks in Figure 6.1. The free boundary is the Mach stem. The endpoints are known, as they are the points where the incident shock meets the sonic circle. The evolution equation for the shock is

$$\frac{d\eta}{d\xi} = \frac{-\xi\eta + \sqrt{s^2(\xi^2 + \eta^2 - s^2)}}{s^2 - \xi^2} = \frac{\eta^2 - s^2}{\xi\eta + \sqrt{s^2(\xi^2 + \eta^2 - s^2)}}. \quad (6.10)$$

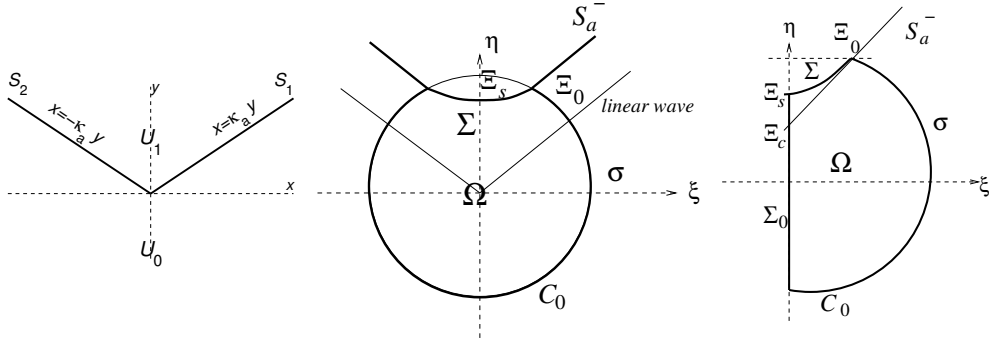


FIGURE 6.1: Data and the Subsonic Region for Weak Mach Reflection

Here $s = s(\rho, \rho_1) = \sqrt{(p(\rho) - p(\rho_1))/(\rho - \rho_1)}$; see Example 4.6 for the original equations. The oblique derivative boundary condition is

$$Mu \equiv \beta \cdot \nabla u = 0 \quad (6.11)$$

on Σ , with

$$\begin{aligned} \beta_1 = & (\xi^2 + \eta^2)(-\eta'\xi + \eta)(c^2(\rho) + s^2(\rho, \rho_1)) \\ & - 2s^2 \{-\eta'\xi(c^2 + \eta^2) + (1 - (\eta')^2)\eta(c^2 - \xi^2) + \eta'\xi(-c^2 + \xi^2)\}, \end{aligned} \quad (6.12)$$

and

$$\begin{aligned} \beta_2 = & \eta'(\xi^2 + \eta^2)(-\eta'\xi + \eta)(c^2(\rho) + s^2(\rho, \rho_1)) \\ & - 2s^2 \{\eta'\eta(c^2 - \eta^2) + (1 - (\eta')^2)\xi(c^2 - \eta^2) + \eta'\eta(c^2 + \xi^2)\}. \end{aligned} \quad (6.13)$$

The boundary operator M is not oblique at the symmetry axis Ξ_s . Rather than deal with a problem where obliqueness fails at an interior point, we have solved the problem on the half domain $\Omega \cap \{\xi > 0\}$ and used the symmetry of the problem to impose the boundary condition $\rho_\xi = 0$ on the vertical axis. Hence the Neumann boundary is $\Sigma_0 = \{\xi = 0, \eta \geq -c_0\}$. The upper end of this boundary is the Mach stem, unknown a priori; however it is clear that the boundary Σ_0 and the boundary condition there can be extended along the positive η axis. The Dirichlet boundary in this example consists of a single point, the intersection of Σ and Σ_0 . This is a little surprising, but is a classic property of mixed boundary conditions of the type we have here.

EXAMPLE 6.4 In [52], Zheng considers data for the pressure-gradient system, (4.12), introduced in Example 4.7, with data constant in four sectors, as shown in Figure 6.2. The data is chosen so that the only nonlinear waves are two shocks moving downward, as sketched on the right side of the figure. By contrast with Example 6.3, the curved shock in this problem decays in strength between the

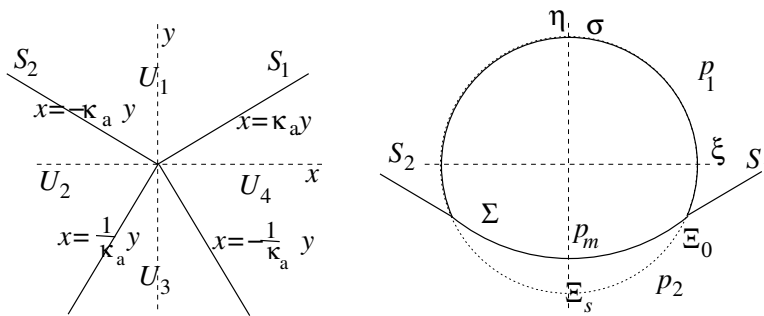


FIGURE 6.2: Symmetric Shock Interaction in the Pressure-Gradient System

formation point Ξ_0 and the symmetry point Ξ_s , and it is probable that for κ_a sufficiently small the shock becomes a weak (linear) wave before it reaches the symmetry axis. Zheng shows that for sufficiently large κ_a a solution exists. He uses a somewhat different technique from ours. By taking the symmetry point Ξ_s and hence p_m , the value of p at the axis, as given, with $p_2 < p_m < p_1$, he shows that a subsonic solution exists, solving the free boundary problem from the axis to the sonic circle, and then determines κ_a from the slope of Σ at Ξ_0 .

EXAMPLE 6.5 Another problem on which we have made some progress concerns regular reflection patterns in the UTSD equation. One expects regular reflection to appear for large values of the parameter a (the slope of the incident shock $x = ay$ in Figure 6.3; note that the wall is horizontal in this problem, whereas it was vertical in the nonlinear wave system example). There are two types of regular reflection: ‘weak’, where a supersonic region appears just beyond the shock reflection, and ‘strong’, with the region right beyond the reflection point already subsonic. In the case of strong reflection, the equation is strictly elliptic in the closure of the subsonic region. In either case, because the subsonic region is unbounded, we impose an artificial cutoff, a curve σ_0 on which we place a Dirichlet condition. Figure 6.3 illustrates the ‘weak’ case. The ξ axis is a symmetry axis, on which a homogeneous Neumann condition is posed. The shock is again a free boundary. In the strong reflection case, the free boundary begins right at the known reflection point, so again the initial position is known. Again in this case a one-point Dirichlet condition must be imposed in order to obtain a nontrivial solution. The condition is given at the known reflection point Ξ_a and consists of the value of the solution just beyond the reflection point, known from the shock polar. Thus, the Dirichlet boundary has two components in ‘strong’ regular reflection. In ‘weak’ reflection, Figure 6.3, there is in addition a sonic boundary along which the solution is continuous, since the constant reflected state changes from supersonic to sonic as one travels away from the reflection point. The intersection Ξ_0 of the reflected shock with this boundary marks the beginning of the free boundary, and serves as the initial condition for the free boundary position. The Dirichlet and Neumann boundaries are the same as in

noting that u still needs to be evaluated on the old boundary Σ in order for the function f to be well-defined.

The fact that the mapping is defined by an integral motivates the use of Hölder spaces and the following version of the Schauder Fixed Point Theorem:

THEOREM 6.6 ([28, Corollary 10.2]) *Let \mathcal{K} be a closed, convex subset of a Banach space \mathcal{B} and let J be a continuous mapping from \mathcal{K} into itself such that the image $J\mathcal{K}$ is precompact. Then J has a fixed point.*

To apply this theorem, we proceed as follows. First, we note that there are two levels of difficulty, depending on whether the problem contains a degenerate boundary or not. We recall that, even though the basic equation changes type, it may happen that this change of type occurs only across shocks (as in strong transonic regular reflection, or steady transonic shock perturbation, for example) and that the elliptic equation is uniformly elliptic (or rather, can be modified to be so, using realistic cutoff functions). In this case, we solve the free boundary problem in four steps:

STEP 1: Fix an approximate position for the free boundary, Σ , given by $\eta = \eta(\xi)$, which defines $\Sigma \in \mathcal{K}$, a subset of a Hölder space $H_{1+\alpha_\Sigma}$. Here α_Σ denotes the Hölder exponent of Σ . We identify a suitable value for α_Σ in Section 7.2, equation (7.4).

STEP 2: Solve a (fixed) mixed boundary value problem for the key variable, u , using Lieberman's theory for mixed boundary value problems in Lipschitz domains. This step typically involves solving the quasilinear problem through linearization, and another application of a fixed point theorem. It may also be necessary to introduce modifications for loss of obliqueness in the derivative boundary condition.

STEP 3: Map $\eta \rightarrow \tilde{\eta} = J\eta$ by the shock evolution condition (the other Rankine-Hugoniot condition); show that the image $J\mathcal{K}$ is precompact and invoke Theorem 6.6. Specifically, we show that J maps $\mathcal{K} \subset H_{1+\alpha_\Sigma}$ to $\mathcal{K} \cap H_{1+\alpha}$, for some $\alpha > \alpha_\Sigma$.

STEP 4: Show that the fixed point η and the corresponding solution u solve the problem (typically straightforward).

However, in many interesting problems one expects the equation to be degenerate elliptic on a portion of the boundary, as in Example 6.3. (It is also possible to pose problems in which the entire boundary is degenerate. A problem of this type with a fixed boundary was first solved by Zheng, [50]. Example 5.1 poses a problem with a degenerate boundary which is also a free boundary.) In this case, we have made progress by applying an elliptic regularization to the operator Q , and using the four-step process above on Q^ε . Additional estimates are required to take the limit $\varepsilon \rightarrow 0$. The overall process consists of four parts.

PART 1: Prove existence, as above, for the free boundary problem with Q replaced by Q^ε ; derive a priori bounds, uniform in ε , on u^ε and $\eta^\varepsilon(\xi)$.

PART 2: Obtain local lower barriers for u^ε , which are independent of ε and imply uniform local ellipticity. The key point here (first recognized by Zheng [50] in this context) is that the actual solution to the degenerate problem is strictly elliptic away from the boundary.

PART 3: Obtain convergent subsequences $\{u^{\varepsilon_i}\}$ and $\{\eta^{\varepsilon_i}\}$ making use of regularity, compactness (from the local ellipticity) and a diagonalization.

PART 4: Show that the limit u solves the problem. This part may require significant work. In passing to a subsequence in the previous part, important information about a priori estimates is lost.

For \mathcal{B} in Theorem 6.6, we choose a Hölder space $H_{1+\alpha_\Sigma}[a, b]$, and the closed set \mathcal{K} is specified, as in Definition 7.6, by $\eta(a) = \eta_0$ and by $f_m \leq \eta' \leq f_M$. Working in Hölder spaces is also compatible with existing theories for oblique derivative boundary conditions, and for ‘mixed’ problems of the type we solve here, with different boundary conditions on different parts of the boundary.

Now, the existence of corners appears to be a basic property of the subsonic domain Ω , with a consequent loss of regularity of solutions there. One of the mechanisms for obtaining compactness of the mapping J is the knowledge that u in the integrand of equation (6.15) is the value on Σ of a function defined there by its derivative; and we use in an essential way the improvement in regularity that one gets in solving elliptic problems with derivative type boundary conditions. It is also standard, following the work of Lieberman and others [39, 41], that this improvement in regularity (known as Schauder or boundary gradient estimates) persists even when corners are present, as they typically are with mixed type boundary conditions. This is dealt with by the use of *weighted Hölder spaces*, defined following Lieberman [39, 41].

We recall the definitions of Hölder norms. Let $X = (\xi, \eta)$; let $D = (D_1, D_2)$ denote partial derivatives, and $D^k u$ the set of k -th order derivatives. For functions defined on an open set Ω in \mathbb{R}^n , the supremum norm and Hölder semi-norms are

$$|u|_{0;\Omega} = \sup_{X \in \Omega} |u(X)| \quad \text{and} \quad [u]_{\alpha;\Omega} = \sup_{X, Y \in \Omega} \frac{|u(X) - u(Y)|}{|X - Y|^\alpha}$$

for $0 < \alpha \leq 1$. Hölder norms of any order are defined by

$$|u|_{\alpha;\Omega} = |u|_{0;\Omega} + [u]_{\alpha;\Omega} \quad \text{for} \quad 0 < \alpha \leq 1,$$

and, for $a = k + \alpha$ where k is an integer and $0 < \alpha \leq 1$,

$$|u|_{a;\Omega} = \sum_{j < k} |D^j u|_{0;\Omega} + |D^k u|_{\alpha;\Omega}.$$

The space of functions whose $(k + \alpha)$ -Hölder norm is finite is denoted $H_{k+\alpha}$. For $\Sigma = \{(\xi, \eta(\xi)) \mid a < \xi < b\}$, we say $\Sigma \in H_{1+\alpha}$ if $\eta \in H_{1+\alpha}(a, b)$. We let $\mathbf{V} = \{V_1, \dots, V_j\}$ denote the set of corners of Ω . Weighted or partially interior seminorms are defined as follows. For a subset S (which is often \mathbf{V} in our case) of $\partial\Omega$, define

$$\Omega_{\delta;S} = \{X \in \Omega \mid \text{dist}(X, S) > \delta\}.$$

DEFINITION 6.7 *For any $a > 0$ and $a + b \geq 0$, the weighted Hölder norm of u on a domain Ω with respect to boundary component S , with complement S^c in $\partial\Omega$, is*

$$|u|_{a;\Omega \cup S^c}^{(b)} = \sup_{\delta > 0} \delta^{a+b} |u|_{a;\Omega_{\delta;S}}. \quad (6.17)$$

The set of functions on Ω with finite norm $|u|_{a;\Omega \cup S^c}^{(b)}$ is denoted $H_{a;\Omega \cup S^c}^{(b)}$.

With $S = \mathbf{V}$, we have $S^c = \Sigma \cup \Sigma_0 \cup \sigma \cup \sigma_0 = \partial\Omega \setminus \mathbf{V}$ and we define $H_a^{(b)} = H_{a;\Omega \setminus \mathbf{V}}^{(b)}$. (By convention, each boundary component is relatively open.) These spaces measure the loss of regularity we expect to find at corners. For example, the function r^γ , with r measuring distance from a corner, is in $H_a^{(-\gamma)}$ for $a \geq \gamma$.

These spaces have a compactness property: for $0 < b' < b$, $0 < a' < a$, $a \geq b$ and $a' \geq b'$, a bounded sequence in $H_a^{(-b)}$ is precompact in $H_{a'}^{(-b')}$ [27, Lemma 4.2].

There are two parts to the program: first, constructing a fixed point of a mapping, assuming we are dealing with a uniformly elliptic equation, Steps 1–4, and then obtaining a solution of the problem by letting the regularizing parameter tend to zero, Parts 1–4. We consider these in turn. In Section 7, we suppose that the operator Q is uniformly elliptic.

7 EXISTENCE OF A SUBSONIC SOLUTION: THE UNIFORMLY ELLIPTIC CASE

In this section, we outline how Steps 1–4 are handled. We use the notation established in equations (6.5), (6.8), (6.6), (6.7) and (6.9). The method for solving the boundary value problem posed in these equations depends on the Schauder theory which provides interior and boundary estimates on solutions of linear elliptic equations.

One way in which elliptic estimates differ from the types of bounds one obtains in hyperbolic equations is that linear estimates are the key; once an estimate is obtained for a linearized equation, existence for the nonlinear equation usually follows from a compactness argument. In particular, this means that there is typically no restriction to data of small oscillation. A second important property is that regularity of solutions and bounds on solutions tend to be independent of bounds on and regularity of the coefficients of the equation; this is the key to obtaining compactness when solving a nonlinear problem as a sequence of linear ones.

The Schauder theory is expounded in detail in Gilbarg and Trudinger’s monograph [28, Chapters 6 and 10]; for extensions to oblique derivative problems, the reference is papers of Lieberman, for example [39, 41].

7.1 L^∞ BOUNDS AND MONOTONICITY

In the problems we have succeeded in solving, there are natural bounds on the position of the free boundary, and with those bounds come natural upper and lower bounds on the nonlinear variable u .

EXAMPLE 7.1 In Example 6.5, regular reflection in the UTSD equation, the free boundary Σ lies between two parabolas, P_1 through $(1, 0)$ and a translated parabola P_a through Ξ_a , pictured in Figure 6.3. We have Dirichlet data on σ and σ_0 , and homogeneous oblique derivative boundary conditions on Σ and Σ_0 , which bound u between $\min_{\sigma_0} u$ and $u|_\sigma$. In Example 6.1 for the nonlinear wave system, the curve Σ lies between the straight line continuation of the incident shock and the horizontal line through Ξ_0 , Figure 6.1. Again, we have homogeneous boundary conditions on Σ and Σ_0 . This time, the lower bound is $u = u_0$ on σ while the upper bound, $u(\Xi_s)$ is bounded below and above by the limiting conditions, $u(\Xi_c) = u_0$ (corresponding to the unphysical case of a constant subsonic state), and a maximum determined from the Rankine-Hugoniot condition for a horizontal shock through Ξ_0 .

EXAMPLE 7.2 We describe a situation in which bounds are less tractable. In setting up the conditions for weak Mach reflection in Example 6.1, we required κ_a to be large enough that the incident shock S intersected the sonic circle $\xi^2 + \eta^2 = c_0^2$ at a point (ξ_0, η_0) with $\xi_0 > 0$. The values of κ_a for which this occurs depend on the ratio ρ_0/ρ_1 . In examining the types of shock interaction which may occur, there appear to be three possibilities. First, the incident shock S_1 and its mirror image S_2 in Figure 6.1 may intersect C_0 before they intersect each other (large κ_a). (This geometric condition defines *Region A** in Figure 7.1.) At the other extreme, they may intersect each other high enough on the η axis that the quasi-one-dimensional Riemann problem so formed has a solution (small κ_a ; *Region C* in Figure 7.1). There is a region between these two cases, *Region B*, where neither alternative holds. We discuss *Region C* in Example 7.7, below. A conjecture for the solution in *Region B* was discussed in Example 5.3. Figure 7.1 gives two views of the regions: the first is a bifurcation diagram parameterized by the quantities κ_a , ρ_0 and ρ_1 which define the Riemann data for this problem. On the right, we present the same regions, parameterized by the angle the incident shock makes with the vertical rather than by κ_a . To the extent that the NLWS provides a model for gas dynamics, this parameter represents the angle of the wedge in the problem of shock reflection by a wedge, while ρ_0/ρ_1 is proportional to the Mach number. This diagram represents the familiar transition between

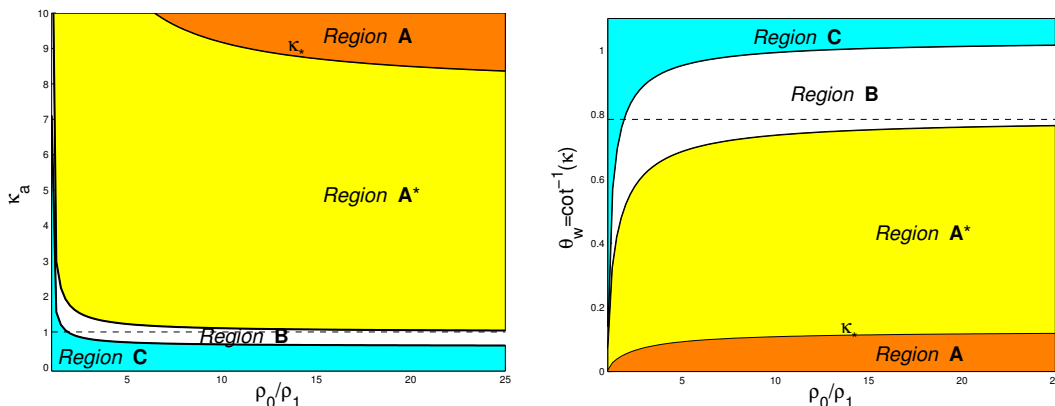


FIGURE 7.1: Shock Reflection in the NLWS: Bifurcation Diagram

regular and Mach reflection. That there is a region in which no solution of either kind appears to exist is an example of the von Neumann paradox.

In fact, as will be described in Section 8, we actually require $\kappa > \kappa_*$, a value whose existence is stated as Lemma 8.5. The estimate we found in [13] in proving Lemma 8.5 is not sharp; however, numerical simulations indicate that the solution described in Example 6.3 and illustrated in Figure 6.1 does not persist up to the curve separating *Region A** from *Region B*. A second type of solution, which appears in simulations, contains a reflected shock which forms with zero strength at the point Ξ_0 , and then grows to a shock of finite strength and either decays again to zero strength, at or before the bottom of the sonic circle, or forms a roughly circular reflected shock. In this case, we have not yet found bounds for the position or maximum strength of the reflected shock. The next example formulates a problem for a more symmetric version of this kind of reflection, where bounds could be established.

EXAMPLE 7.3 The equation is again the nonlinear wave system; the data are chosen with $\rho_0 = \rho_1 = \rho_2$ and so that shocks of identical strength move away from the initial discontinuities, both up and down. See Figure 7.2. (There is a two-parameter family of data that leads to this symmetric configuration.) The conjectured solution contains three Mach stems, with positions and maximum values of ρ as in Example 7.1, and three reflected shocks. This problem contains six free boundary segments of two types, but each can be handled independently of the others. The solution is still sonic — degenerate elliptic — at Ξ_0 and at the five images of this point under reflection and rotation. In this case, we conjecture that the maximum value of u along the reflected shock occurs at the mid-point, Ξ_m in Figure 7.2, which is also the point at which the derivative condition is not oblique. In solving this problem by the fixed point method, this point is part of the Dirichlet boundary, as in equation (6.9). In fact, the initial angle of the

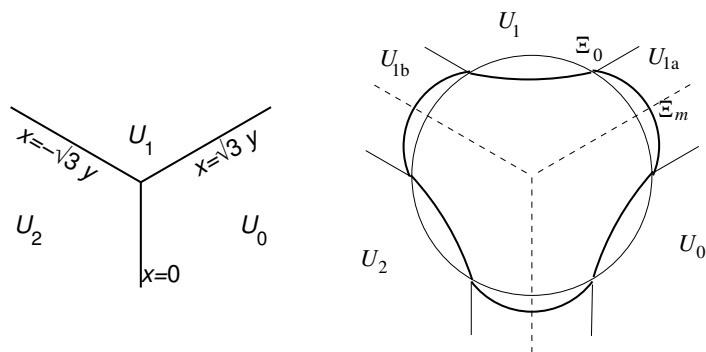


FIGURE 7.2: A Symmetric Mach Reflection Problem

reflected shock is known (tangent to the sonic circle), and if we suppose that the reflected shock is convex, then this gives an outer bound for the point Ξ_m , and hence, using the Rankine-Hugoniot conditions and knowing the shock angle by symmetry, an upper bound for ρ . Based on numerical evidence that the reflected shock is close to the sonic circle, these bounds are not very sharp, and it is not clear that they will be sufficient to prove a theorem in this case.

It is often not difficult to show that a Mach stem or reflected shock is a convex curve, and that the significant variable, u , is monotonic along the shock. This can be seen, much of the time, from the Rankine-Hugoniot conditions. However, our approach requires us to solve fixed boundary problems in which only part of the Rankine-Hugoniot relation holds, and also to update the shock position by invoking the complementary Rankine-Hugoniot relations, thereby producing a region in which the partial differential equation does not hold. Specifically, the fixed mixed boundary value problem has the form (6.16). It turns out that one can often infer both L^∞ bounds on the solution and monotonicity along the approximate shock boundary even without having a complete solution. One form of the result is

PROPOSITION 7.4 *Consider a solution $u \in C^1(\Omega \cup \Sigma \cup \Sigma_0) \cap C(\overline{\Omega})$ of the fixed mixed boundary value problem (6.16). Suppose that u is elliptic in Ω , that $g = 0 = \psi$ and that ϕ is constant. Assume further that each component of both Σ and Σ_0 terminates at points which are in the closure of $\sigma \cup \sigma_0$. Then, the maximum of u in Ω is achieved on σ_0 and u is monotonic on Σ and on Σ_0 .*

PROOF: We sketch the proof; a complete proof in a particular case is given in [13, Proposition 2.4]. The regular and Hopf maximum principles apply to an operator of the form Q . If the extrema of u are attained at points on the boundary other than in $\sigma_0 \cup \sigma$, then the tangential derivatives of u along $\partial\Omega$ are zero there. By the homogeneous boundary conditions, then, the gradient of u is zero at such a point, and this contradicts the Hopf maximum principle. Thus the extrema of u in $\overline{\Omega}$ are attained on $\sigma \cup \sigma_0$.

Monotonicity requires a more subtle argument. We note first that if u is not monotonic on either curve then u , restricted to that curve, has both a local maximum and a local minimum along that curve. By the Hopf maximum principle, neither of the extrema along the curve is a local extremum in Ω . Hence one can find a curve in Ω which leaves the maximum, along which u is increasing, and a curve from the minimum along which u decreases. Following these curves results in a contradiction. ■

One can consider extensions of this principle to non-homogeneous derivative boundary conditions and non-constant Dirichlet conditions. For some problems, convexity of the shock curve can also be seen easily.

EXAMPLE 7.5 Consider the Mach stem in the nonlinear wave system, Example 6.1 and 6.3. The shock position satisfies

$$\eta' = f(\xi, \eta(\xi), \rho(\xi, \eta(\xi))),$$

and so

$$\eta'' = f_\xi + f_\eta \eta' + f_\rho \rho'.$$

However, $f_\xi + f_\eta \eta' = 0$ (since constant ρ leads to a straight line shock). A calculation shows that $f_\rho \leq 0$, while monotonicity of ρ along the shock, Proposition 7.4, gives $\rho' \leq 0$, whence $\eta'' \geq 0$.

The reflected shock in the UTSD equation, Example 6.5, is convex by the same argument. To apply Proposition 7.4 here, we must take the Dirichlet data to be constant on the cutoff boundary σ_0 . Then $u(\eta)$ is monotonic along the shock $\xi(\eta)$. From the shock equation

$$\frac{d\xi}{d\eta} = f(\xi(\eta), \eta, u(\xi(\eta), \eta)) = -\frac{\eta}{2} - \sqrt{\xi + \frac{\eta^2}{4} - \frac{u+1}{2}}, \quad (7.1)$$

we obtain $f_u \geq 0$ and $\xi'' \leq 0$. Hence the shock is convex.

7.2 THE FIXED POINT OF THE MAPPING

The basic mapping is (6.14), (6.15). We define a bounded convex set \mathcal{K} using bounds like those in Example 7.1.

DEFINITION 7.6 *The set \mathcal{K} is defined by two sorts of conditions:*

- (K1)** *Analytic:* $\mathcal{K} \subset H_{1+\alpha_\Sigma}(a, b)$;
- (K2)** *Geometric:* $\eta(a) = \eta_0$; $f_m \leq \eta' \leq f_M$.

Here f_m and f_M are lower and upper bounds on $f(\xi, \eta, u)$ (which may in turn depend on a priori bounds on u). In addition, it may be convenient to impose other geometric constraints; this has been the case in the examples we have solved.

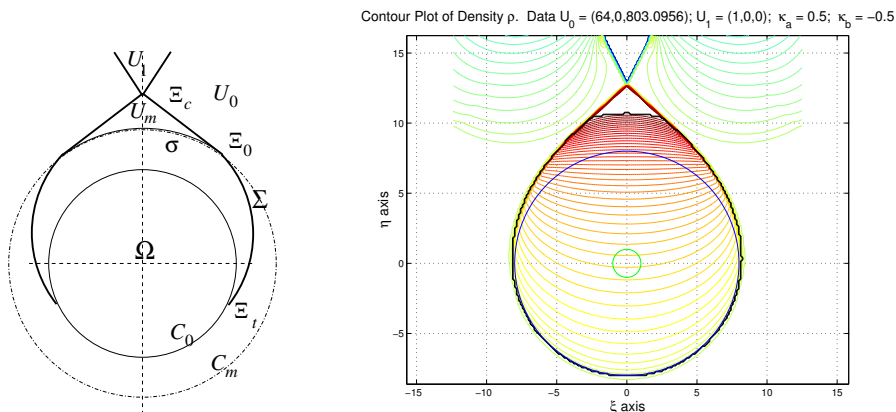


FIGURE 7.3: Regular Reflection: Sketch and Simulation (Kurganov)

We note a recurring difficulty: The equation for the shock angle is nonlinear; see (6.3), (6.10) or (7.1) for example. Hence the function f is typically defined only for some values of u . One resolution of this difficulty is to modify f with a cutoff function, and then to attempt to remove the cutoff. For the UTSD equation, Example 6.5, we were unable to remove the cutoff completely, and thus we found only a local solution. In the special case of the Mach stem problem we solved for the NLWS, Example 6.3, we were able to show a priori that f was defined for all functions used in the mapping. In the slightly different shock interaction problem for the NLWS (or pressure-gradient system), described in Example 6.4, Zheng [52] encountered the same difficulty as in the UTSD equation; the difficulty also arises in studying regular reflection for the NLWS.

EXAMPLE 7.7 Consider regular reflection in the nonlinear wave system for the data of Example 6.1, this time with κ_a chosen small enough (*Region C* of Figure 7.1) that the incident shocks meet above the sonic circle and that the quasi-one-dimensional Riemann problem at the intersection point Ξ_c has a solution. There are two solutions, corresponding to weak and strong regular reflection. In either case, after the reflected shock becomes transonic, the shock, now represented by $\xi(\eta)$, satisfies an equation like (6.10):

$$\frac{d\xi}{d\eta} = \frac{\xi\eta \pm \sqrt{s^2(\xi^2 + \eta^2 - s^2)}}{\eta^2 - s^2}. \quad (7.2)$$

The reflected shock may terminate at a point Ξ_t where $\rho = \rho_0$, $s = c(\rho_0)$ and $\xi^2 + \eta^2 = c^2(\rho_0)$, on the sonic circle C_0 . (See Figure 7.3 for a sketch and numerical simulation by Kurganov of this problem.) At this point, the quantity under the square root sign in (7.2) is zero. However, the corresponding fixed boundary value problem, (6.16), for a given Σ , will have a solution $\rho(\xi, \eta)$ which does not, of course, satisfy (7.2). There seems to be no a priori way of ensuring that

$\xi^2 + \eta^2 - s^2(\rho, \rho_0)$ will be positive (or nonnegative) for this problem. Thus, the mapping J must be replaced by an equation of the form

$$\frac{d\tilde{\xi}}{d\eta} = \frac{\xi\eta \pm \sqrt{g_\delta(s^2(\xi^2 + \eta^2 - s^2))}}{\eta^2 - s^2},$$

where $g_\delta(X) = X$ for $X \geq \delta > 0$, $g_\delta(X) = \delta$ otherwise. This type of cutoff function was introduced in the regular reflection problem for the UTSD equation, Example 6.5, and we were not able to remove it in [9, 10]. It is even possible, in this problem, the the reflected shock does not terminate but extends completely around the circle.

For the remainder of this exposition, we shall assume that f is defined for all functions in the range we consider. In particular, we may take f to be an analytic function of its arguments.

Following the program outlined in Steps 1–4 of Section 6, we note that checking the hypotheses of Theorem 6.6 involves two parts. First we must establish that any solution of (6.15) satisfies the geometric bounds, **(K2)**. This result is problem-dependent.

EXAMPLE 7.8 For the Mach stem for the NLWS, Example 6.3, a satisfactory set of geometric conditions is given by

$$\eta(\xi_0) = \eta_0, \quad \eta'(\xi_0) = 1/\kappa_a, \quad \eta_c \leq \eta(\xi) \leq \eta_0, \quad 0 \leq \eta' \leq \sqrt{c_0^2/s_0^2 - 1}, \quad (7.3)$$

and in [13] we verified that provided η is monotone and ρ along the curve Σ is monotonic and satisfies $\rho(\xi_0) = \rho_0$, and $s(\rho(\xi_0), \rho(0)) = \eta(0)$, then $\tilde{\eta}$ also satisfies (7.3).

On the other hand, establishing that the Hölder class of $J\eta$ is $H_{1+\alpha}$ for some $\alpha > \alpha_\Sigma$ is the source of the compactness of the mapping, and is the unifying principle of our method. Since $J\eta$ is found by integration, the Hölder class of $J\eta$ is $1 + \alpha_\Omega$, where α_Ω is the Hölder class of the solution u of the fixed mixed boundary value problem (6.16) which we now discuss.

The existence of a solution of this problem, and a priori estimates for it, form the backbone of our approach. The critical step is to obtain bounds on the solution at Σ which are independent of the exponent α_Σ . The estimates for this are derived from basic Schauder theory [28], from Lieberman's work [39, 41], and from estimates due to Gilbarg and Hörmander [27]. We prove

THEOREM 7.9 ([9], THEOREM 4.1; [13], THEOREM 3.7) *Suppose that any solution u of (6.16) satisfies a priori bounds $u \in I$ and that Q is uniformly elliptic and M uniformly oblique for $u \in I$. Suppose that Σ , Σ_0 , σ and σ_0 are all in $H_{1+\alpha_\Sigma}$ and that the corner angles all lie in a range (θ_0, θ_1) . Then (6.16) has a solution $u \in H_{1+\alpha}^{(-\gamma)}$ for all $\alpha \leq \alpha_\Sigma$ and all $\gamma \leq \gamma_V$, where γ_V depends on θ_0 and θ_1 , the ellipticity ratio and the obliqueness ratio.*

For this result, we choose the weighted space to have weights at the set of corners \mathbf{V} , and note that the solution lies in $C_\gamma(\overline{\Omega})$.

This theorem is proved by linearizing, replacing Q and M by linearized operators L and N :

$$Lu = D_i(a_{ij}(\Xi, w)D_j u) + b_i(\Xi)D_i u, \quad Nu = \beta_i(\Xi, w)D_i u,$$

for $w \in \mathcal{W} \subset H_{1+\epsilon}^{(-\gamma_1)}$, where \mathcal{W} includes the L^∞ a priori bounds established for u . The important point is that estimates can be obtained for the linear problem which do not depend on the $H_a^{(b)}$ norm of w . Then existence can be proved using the Schauder fixed point theorem on the linearized problem. The linear estimates are based on results of Lieberman, for example [39, Lemma 1], [40, Lemma 1], and [41, Theorem 1]. The important corner estimates are derived in [39, Lemma 2] and [41, Theorem 2].

Now, from Theorem 7.9 we have $u \in H_{1+\alpha_\Sigma}$ except at the corners, where $u \in H_{\gamma_V}$. Provided f is smooth, we then have $\tilde{\eta} \in H_{1+\alpha}$ for any $\alpha \leq \gamma_V$. Thus if

$$\alpha_\Sigma = \gamma_V/2 \tag{7.4}$$

we have a compact mapping and Theorem 6.6 gives the fixed point.

At this point, we discuss the possible failure of obliqueness. In some of the problems we have studied, the derivative operator, $M = \beta \cdot \nabla$ loses obliqueness at points where $f = 0$. These correspond to symmetry points, for example where a shock hits the wall, or where it changes from a '+' to a '-' shock. It seems likely that this loss of obliqueness is generic, and will occur at isolated points on most transonic shocks. Since all the estimates used in Theorem 7.9 depend on the obliqueness ratio, loss of obliqueness is a serious difficulty. The linearization procedure can be carried out; in fact, it is typically not difficult to modify the derivative operator to make it uniformly oblique, and to obtain a convergent sequence which solves the linear problem. However, obtaining linear estimates, needed to solve the nonlinear problem, is more difficult. This was handled in [13] by modifying the procedure outlined above.

1. We replaced the weights at corners by a weight along $\overline{\Sigma}$; thus the set S in the definition of the norm of u , equation (6.17), is now $\Sigma \cup \mathbf{V}$.
2. We found a solution to the nonlinear problem in $H_{2+\alpha}^{(-\gamma)}(\Omega)$ which satisfied an additional bound, $|\rho|_{\gamma; \Sigma(d_0)} \leq K_1$, where $\Sigma(d_0)$ is a neighborhood of $\overline{\Sigma}$ and K_1 , like γ , is independent of α_Σ . This, as in Theorem 7.9, was enough to give a fixed point.

In [34], Kim has shown that the procedure in [13] works quite generally when obliqueness fails.

Another feature of our approach is that the regularity which we assume for Σ , which is less than $2 + \alpha$, is lower than the boundary regularity assumed in

the results quoted above. Following Lieberman [38], we introduced a regularized distance function (or regularized domain). For all the estimates we need, this has proved adequate.

Once a fixed point of J has been found, the pair (u, η) gives a solution to the free boundary problem.

8 THE DEGENERATE ELLIPTIC FREE BOUNDARY PROBLEM

We now summarize how we handle the case that there is a component of the boundary, σ , on which Q is degenerate elliptic and u is constant. We follow the four parts outlined in Section 6.

The first part is to replace Q by $Q^\varepsilon = Q + \varepsilon\Delta$. The problem can now be handled by the method of Section 7. We obtain a solution $(u^\varepsilon, \eta^\varepsilon)$ for each $\varepsilon > 0$ which lies in

$$C^{2+\alpha}(\overline{\Omega^\varepsilon} \setminus S^\varepsilon) \cap C^\alpha(\overline{\Omega^\varepsilon}) \times C^{2+\alpha}(a, b),$$

where $\alpha = \alpha(\varepsilon)$ and $S^\varepsilon = \mathbf{V}$ or $\Sigma^\varepsilon \cup \mathbf{V}$.

We see immediately that the sequence $\{\eta^\varepsilon\}$ is uniformly bounded and equicontinuous, from the geometric bounds **(K2)** on the set \mathcal{K} , which are independent of ε . Hence the Arzelà-Ascoli theorem implies existence of a convergent subsequence $\eta^i \rightarrow \eta$. We now restrict attention to that sequence. The limit, η is in $C^\gamma([a, b])$ for all $\gamma \in (0, 1)$, and the sequence of domains Ω^i has a limit Ω .

8.1 LOCAL LOWER BARRIERS AND CONVERGENCE

Now the critical issue is that of uniform ellipticity of the operators Q^ε in compact subsets of Ω .

EXAMPLE 8.1 In the interacting shock problem for the nonlinear wave system, we have $\rho^\varepsilon(\xi, \eta) > \rho_0$ for all $(\xi, \eta) \in \Omega^\varepsilon$, where ρ_0 is the constant boundary value on the degenerate boundary σ . Since the ellipticity ratio is $1 - (\xi^2 + \eta^2)/c^2(\rho)$, (Example 4.10) and c^2 is monotone in ρ , while $c^2(\rho_0) = \xi^2 + \eta^2$ on σ (where, in turn, $\xi^2 + \eta^2$ has its maximum value in Ω), we clearly have

$$1 - \frac{\xi^2 + \eta^2}{c^2(\rho)} \geq \delta > 0$$

on compact subsets of Ω . In fact, the uniform bound holds on any closed subset of $\overline{\Omega} \setminus \overline{\sigma}$.

The analysis in this example is simpler than the typical case, but illustrates the general idea. The objective is to find a lower barrier ϕ , independent of ε , such that we have $u^\varepsilon \geq \phi$ for all ε and such that $\lambda(u) \geq \lambda(\phi) \geq \delta > 0$, where λ is the ellipticity ratio of the principal part of Qu , Definition 4.9. In fact, it is sufficient

to do this locally: Show that on each closed set B in $\overline{\Omega} \setminus \overline{\sigma}$ there is a $\phi = \phi_B$ with this property. This was done by Čanić and Kim for a general class of quasilinear degenerate elliptic equations satisfying a structure condition, [16, Lemma 2.4]. The technique in [16] generalizes an approach found independently by Zheng [50, page 1860, equation (3.7)] and by Choi and McKenna [24, Theorem 3].

Then the following Lemma gives a limit solution u :

LEMMA 8.2 *Suppose that $\{u^i\}$ is a sequence such that Qu^i is uniformly elliptic on each closed subset of $\overline{\Omega} \setminus \overline{\sigma}$, with ellipticity ratio independent of i . Then there is a subsequence which converges to a limit u which is in $C^{2+\alpha}(\Omega)$ for some α .*

This is proved by compactness and diagonalization arguments. The proof was carried out in detail as Lemma 4.2 of [10].

8.2 VERIFICATION OF THE SOLUTION

The compactness argument also shows that the limit function satisfies the equation $Qu = 0$, as was shown by Choi and McKenna [24]. Convergence and continuity up to the Dirichlet and Neumann boundaries is also standard. Uniform ellipticity up to the free boundary Σ also allows us to verify the free boundary conditions.

LEMMA 8.3 ([10], LEMMA 4.3) *The limits u and η satisfy $Mu = 0$ on Σ and $\eta' = f(\xi, \eta(\xi), u(\xi, \eta(\xi)))$.*

The convergence in Lemma 8.2 and the proof of Lemma 8.3 use uniform obliqueness. At the point where obliqueness failed in the Mach stem problem for the NLWS, we were able to prove this result [13, Lemma 4.4] by observing that the condition $f = 0$, which corresponds to $\eta' = 0$, at the point where obliqueness fails, is satisfied precisely when the one-point Dirichlet condition holds. Kim has shown that whenever the tangential derivative implies a Dirichlet condition then this procedure works [34, Condition **C** and Lemma 3.9].

8.3 CONVERGENCE AT THE DEGENERATE BOUNDARY

When the subsonic region contains a degenerate boundary and a free boundary which meet at a corner, we have been able to get results only on a case-by-case basis.

In general, as described in Section 4.1, we conjecture that solutions at the degenerate boundary σ will display either linear (square root singularity) or nonlinear behavior (Lipschitz continuous with fixed Lipschitz constant). Specifically, for the examples we have studied and more generally under the structure conditions established in [16], when $u|_{\sigma}$ is a (local) minimum of u in Ω , we see linear behavior; when u is a (local) maximum, the solution is nonlinear. Physically, this may correspond to formation of a weak compression wave on the sonic line

in the linear case, or to a nonlinear perturbation of a subsonic solution. Again, physically, this seems to be determined by the nature of the phenomenon. In the case of interacting shocks, Examples 6.1 and 6.3, the incident shocks interact with each other in the subsonic region, beginning at the sonic line, to produce a Mach stem and a reflected shock. By contrast, in weak regular reflection, Example 6.5, the reflected shock merely crosses the sonic line in the course of becoming transonic, and does not interact with another wave. We classify the former behavior as linear, the latter as nonlinear.

This division is incomplete, at present. In Zheng's example, Example 6.4, the sonic line is a maximum for ρ and we expect nonlinear (Lipschitz) behavior there. (This has not yet been proved.) A physical explanation for why these shocks interact only nonlinearly might involve the fact that the shocks are diverging and hence there is no compression.

In the case of nonlinear behavior, estimates at σ are straightforward.

EXAMPLE 8.4 Consider behavior at σ in the weak regular reflection problem for the UTSDE. The approximate solutions $\{u^\varepsilon\}$ are bounded above by the constant reflected state, u_M , and below by the requirement that the solution be subsonic, so $u(\xi, \eta) > \xi + \eta^2/4$. Since $u_M = \xi + \eta^2/4$ on σ , we see that u is continuous on $\bar{\sigma}$.

In the linear case, when the set $\{u^\varepsilon\}$ is not uniformly Lipschitz, there is more to prove. For a general class of degenerate equations, including all the examples considered in this paper, Čanić and Kim established that the approximate solutions converge at σ to a continuous function [16]. Lemma 3.2 of [16] constructs a (singular) upper barrier function locally at each point in the interior of σ , again following the technique originally developed by Choi, Lazer and McKenna [23, 24]. However, obtaining continuity at the corner Ξ_0 between the degenerate boundary and the free boundary requires an additional hypothesis. For the interacting shock problem for the NLWS, Example 6.3, we were able to prove

LEMMA 8.5 *There is a function $\kappa_*(\rho_1, \rho_0)$ of the Riemann data such that for any $\kappa_a > \kappa_*$ the limit ρ is continuous on $\bar{\Omega}$.*

This lemma was proved using a modification of the singular barrier construction developed in [16], and uses the particular structure of the characteristic and shock speeds in the NLWS. The curve κ_* is sketched in Figure 7.1 for a particular choice of gas law relation. While it is plausible that similar structure relations would allow a version of this result for a wider class of problems, the result is neither general nor sharp, and many open problems remain here.

9 THE SOLUTION OF THE SELF-SIMILAR SYSTEM

At the beginning of Section 6, we outlined the features of self-similar systems that appear to make them amenable to our approach. At this point, we have

outlined how we can set up and under certain conditions solve the free boundary problems for second-order quasilinear elliptic equations which arise. In certain cases, it is then possible to complete the problem by solving for the remaining variables in the original self-similar system. In particular, for the nonlinear wave system, Example 4.6, the second and third equations in the system (4.10) are simply transport equations for the momentum components m and n along radial lines through the origin, and once ρ is known then m and n can be found by integration. Introducing a radial variable $r = \sqrt{\xi^2 + \eta^2}$ gives

$$\frac{\partial m}{\partial r} = \frac{1}{r}p(\rho)_\xi, \quad \frac{\partial n}{\partial r} = \frac{1}{r}p(\rho)_\eta. \quad (9.1)$$

Carrying out the integration from points near infinity (in the hyperbolic region), which is consistent with the time-evolution of (4.10), one obtains a solution in the punctured plane. At the origin, there may be logarithmic singularities in (m, n) . In addition, since at σ we proved only that ρ is continuous, we obtain only weak solutions to (9.1) there, in the sense of distributions. However, irrespective of singularities, we have

PROPOSITION 9.1 *For the nonlinear wave system, the function $U = (\rho, m, n)$ found by solving the free boundary problem for ρ and (9.1) for m and n satisfies the system (4.10).*

PROOF: We need only verify the first equation of (4.10). For this we note that the second order equation for ρ , (4.11), can be written

$$(p(\rho)_\xi - \xi^2\rho_\xi - \xi\eta\rho_\eta)_\xi + (p(\rho)_\eta - \eta^2\rho_\eta - \xi\eta\rho_\xi)_\eta + \xi\rho_\xi + \eta\rho_\eta = 0.$$

Using (9.1), $p_\xi = rm_r = \xi m_\xi + \eta m_\eta$ and $p_\eta = rn_r = \xi n_\xi + \eta n_\eta$, we have

$$(\xi m_\xi + \eta m_\eta - \xi^2\rho_\xi - \xi\eta\rho_\eta)_\xi + (\xi n_\xi + \eta n_\eta - \eta^2\rho_\eta - \xi\eta\rho_\xi)_\eta + \xi\rho_\xi + \eta\rho_\eta = 0. \quad (9.2)$$

Define $R = \xi\rho_\xi + \eta\rho_\eta - m_\xi - n_\eta$. Then, after manipulating derivatives, (9.2) becomes

$$\nabla \cdot R + R = 0. \quad (9.3)$$

That is to say, R is transported on radial lines following (9.3). But now $R = 0$ for sufficiently large (ξ, η) , where the hyperbolic system is satisfied. Hence $R \equiv 0$ and (4.10) is satisfied. ■

Similarly, in the pressure-gradient system, Example 6.4, the first two equations in the system (4.12), written in self-similar coordinates, are transport equations for u and v . We note that such is not the case for the UTSD equation, Example 4.4. Here the self-similar system (4.5) does contain a second equation for v , but it is not a transport equation, for the reasons discussed in Section 4.2. In particular, a solution analogous to the reflected weak compression wave of Example 6.3 does

not exist for the UTSD system, as the solution which could be constructed for u cannot be extended to v without creating a singularity in v along the entire negative ξ axis. It is conjectured that for this equation the reflected shock is always a genuine shock. That is, no weak compression waves exist for the UTSD system. Whether there might exist a solution in which the reflected shock has strength zero at the formation point, as in Example 7.2, or if all solutions contain embedded supersonic regions, as in Example 5.3, remains an open question.

10 ACKNOWLEDGEMENTS

This research is part of a joint project with Sunčica Čanić, and much of it has been carried out with Eun Heui Kim. We have benefited greatly from the advances in Schauder theory made by Gary Lieberman, and from his help in adapting this theory to elliptic problems arising from conservation laws. It is a pleasure to acknowledge the contribution of David Wagner in setting the initial direction of the program, and of conversations with John Hunter, Esteban Tabak and Reuben Rosales about their related work on the UTSD equation. Cathleen Morawetz has given us tremendous encouragement, and many insights into the analytical nature and physical interpretation of shock reflection patterns. We have been fortunate in attracting the interest of several people who have assisted us with computations on the NLWS, including Maria Lukačova, Manuel Torrilhon, Richard Sanders and especially Alexander Kurganov, some of whose results appear in this paper. I also gratefully acknowledge the support and hospitality of the Isaac Newton Institute for Mathematical Sciences at the University of Cambridge, where part of this research was performed in 2003, during the Semester Program “Nonlinear Hyperbolic Waves in Phase Dynamics and Astrophysics” organized by C. M. Dafermos, P. G. LeFloch, and E. F. Toro. Finally, this project is continuing under the auspices of the NSF FRG on Multidimensional Conservation Laws.

NOTE ADDED IN PROOF:

The condition that the solutions of the second-order equation $Qu=0$ of equation (6.5) in the subsonic region give rise to a weak solution in an open set containing the sonic line is that a characteristic form involving the first derivatives of u vanish at the sonic line. This condition holds if the solution is Lipschitz or if the equation is linear, but fails for the singular solution of a quasilinear equation, like the solution illustrated in Example 4.11. In particular, in Examples 7.2 and 7.7, we conclude that for the subsonic flow to be part of a weak solution, the shock does not terminate. On the other hand, in Example 6.1 and 6.3, the degenerate boundary cannot consist of more than a single point (the formation point of the Mach stem), and we conjecture that the full solution requires a second, reflected shock, as in Example 7.3, although numerical simulations appear to give the

solution described in Example 6.1. This phenomenon may be connection to the discussion of vorticity given in Section 4.2. A revision of our work [13] on Example 6.1 to include the correct reflected shock is in progress.

11 REFERENCES

- [1] M. S. BAOUENDI. Sur une classe d'opérateurs elliptiques dégénérés. *Bulletin de la Société Mathématique de France*, 95:45–87, 1967.
- [2] M. BRIO AND J. K. HUNTER. Mach reflection for the two dimensional Burgers equation. *Physica D*, 60:194–207, 1992.
- [3] S. ČANIĆ AND B. L. KEYFITZ. An elliptic problem arising from the unsteady transonic small disturbance equation. *Journal of Differential Equations*, 125:548–574, 1996.
- [4] S. ČANIĆ AND B. L. KEYFITZ. Oblique shock interactions and the von Neumann paradox. In B. Sturtevant, J. E. Schepherd, and H. G. Hornung, (eds), *Proceedings of the 20th International Symposium on Shock Waves, Volume I*, pages 435–440. World Scientific, Singapore, 1996.
- [5] S. ČANIĆ AND B. L. KEYFITZ. A smooth solution for a Keldysh type equation. *Communications in Partial Differential Equations*, 21:319–340, 1996.
- [6] S. ČANIĆ AND B. L. KEYFITZ. A useful class of two-dimensional conservation laws. In K. Kirchgässner, O. Mahrenholtz, and R. Mennicken, (eds), *Proceedings of ICIAM 95: Supplement 2: Applied Analysis; Mathematical Research, Vol. 87*, pages 133–136. Akademie Verlag, Berlin, 1996.
- [7] S. ČANIĆ AND B. L. KEYFITZ. Quasi-one-dimensional Riemann problems and their role in self-similar two-dimensional problems. *Archive for Rational Mechanics and Analysis*, 144:233–258, 1998.
- [8] S. ČANIĆ AND B. L. KEYFITZ. Riemann problems for the two-dimensional unsteady transonic small disturbance equation. *SIAM Journal on Applied Mathematics*, 58:636–665, 1998.
- [9] S. ČANIĆ, B. L. KEYFITZ, AND E. H. KIM. Free boundary problems for the unsteady transonic small disturbance equation: Transonic regular reflection. *Methods and Applications of Analysis*, 7:313–336, 2000.
- [10] S. ČANIĆ, B. L. KEYFITZ, AND E. H. KIM. A free boundary problem for a quasilinear degenerate elliptic equation: Regular reflection of weak shocks. *Communications on Pure and Applied Mathematics*, LV:71–92, 2002.

- [11] S. ČANIĆ, B. L. KEYFITZ, AND E. H. KIM. Mixed hyperbolic-elliptic systems in self-similar flows. *Boletim da Sociedade Brasileira de Matemática*, 32:1–23, 2002.
- [12] S. ČANIĆ, B. L. KEYFITZ, AND E. H. KIM. Weak shock reflection modeled by the unsteady transonic small disturbance equation. In H. Freistuhler and G. G. Warnecke, (eds), *Proceedings of the Eighth International Conference on Hyperbolic Problems: Theory, Numerics, and Applications*, pages 217–226. Birkhäuser, Basil, 2002.
- [13] S. ČANIĆ, B. L. KEYFITZ, AND E. H. KIM. Free boundary problems for nonlinear wave systems: Interacting shocks. *Submitted*, 2003.
- [14] S. ČANIĆ, B. L. KEYFITZ, AND G. M. LIEBERMAN. A proof of existence of perturbed steady transonic shocks via a free boundary problem. *Communications on Pure and Applied Mathematics*, LIII:1–28, 2000.
- [15] S. ČANIĆ, B. L. KEYFITZ, AND D. H. WAGNER. A bifurcation diagram for oblique shock interactions in the unsteady transonic small disturbance equation. In J. Glimm et al., (eds), *Proceedings of the Fifth International Conference on Hyperbolic Problems: Theory, Numerics, and Applications*, pages 178–187. World Scientific, Singapore, 1996.
- [16] S. ČANIĆ AND E. H. KIM. A class of quasilinear degenerate elliptic equations. *Journal of Differential Equations*, 189:71–98, 2003.
- [17] T. CHANG, G.-Q. CHEN, AND S. YANG. On the 2-D Riemann problem for the compressible Euler equations I. Interaction of shocks and rarefaction waves. *Discrete and Continuous Dynamical Systems*, 1:555–584, 1995.
- [18] G.-Q. CHEN AND M. FELDMAN. Multidimensional transonic shocks and free boundary problems for nonlinear equations of mixed type. *Journal of the American Mathematical Society*, 16:461–494, 2003.
- [19] G.-Q. CHEN AND M. FELDMAN. Steady transonic shock and free boundary problems in infinite cylinders for the Euler equations. *Communications on Pure and Applied Mathematics*, 57:310–356, 2004.
- [20] S. CHEN. A singular multi-dimensional piston problem in compressible flow. *Journal of Differential Equations*, 189:292–317, 2003.
- [21] S. CHEN, Z. GENG, AND D. LI. Existence and stability of conic shock waves. *Journal of Mathematical Analysis and Applications*, 277:512–532, 2003.

- [22] Y. S. CHOI AND E. H. KIM. On the existence of positive solutions of quasilinear elliptic boundary value problems. *Journal of Differential Equations*, 155:423–442, 1999.
- [23] Y. S. CHOI, A. C. LAZER, AND P. J. MCKENNA. On a singular quasilinear elliptic boundary value problem. *Transactions of the American Mathematical Society*, 347:2633–2641, 1995.
- [24] Y. S. CHOI AND P. J. MCKENNA. A singular quasilinear elliptic boundary value problem, II. *Transactions of the American Mathematical Society*, 350:2925–2937, 1998.
- [25] Z. DAI AND T. ZHANG. Existence of a global smooth solution for a degenerate Goursat problem of gas dynamics. *Archive for Rational Mechanics and Analysis*, 155:277–298, 2000.
- [26] E. V. FERAPONTOV AND K. R. KHUSNUTDINOVA. On integrability of 2+1-dimensional quasilinear systems. *Preprint*, 2000.
- [27] D. GILBARG AND L. HÖRMANDER. Intermediate Schauder estimates. *Archive for Rational Mechanics and Analysis*, 74:297–318, 1980.
- [28] D. GILBARG AND N. S. TRUDINGER. *Elliptic Partial Differential Equations of Second Order*. Springer-Verlag, New York, Second edition, 1983.
- [29] J. K. HUNTER AND J. B. KELLER. Weak shock diffraction. *Journal of Wave Motion*, 6:79–89, 1984.
- [30] M. V. KELDYSH. On some cases of degenerate elliptic equations on the boundary of a domain. *Doklady Acad. Nauk USSR*, 77:181–183, 1951.
- [31] J. B. KELLER AND A. BLANK. Diffraction and reflection of pulses by wedges and corners. *Communications on Pure and Applied Mathematics*, IV:75–94, 1951.
- [32] B. L. KEYFITZ AND M. C. LOPES-FILHO. How to use symmetry to find models for multidimensional conservation laws. In E. L. Allgower, K. Georg, and R. Miranda, (eds), *Proceedings of AMS/SIAM Summer Seminar on Exploiting Symmetry in Applied and Numerical Analysis*, pages 273–284. American Mathematical Society, Providence, 1993.
- [33] E. H. KIM. Existence results for singular anisotropic elliptic boundary-value problems. *Electronic Journal of Differential Equations*, 2000(17):1–17, 2000.
- [34] E. H. KIM. Free boundary and mixed boundary value problems for quasilinear elliptic equations: tangential oblique derivative and degenerate Dirichlet boundary problems. *Preprint*, 2004.

- [35] E. H. KIM AND K. SONG. Classical solutions for the pressure-gradient equations in non-smooth and non-convex domains. *Journal of Mathematical Analysis and Applications*, to appear.
- [36] J. J. KOHN AND L. NIRENBERG. Degenerate elliptic-parabolic equations of second order. *Communications on Pure and Applied Mathematics*, XX:797–872, 1967.
- [37] A. KURGANOV, S. NOELLE, AND G. PETROVA. Semi-discrete central-upwind schemes for hyperbolic conservation laws and Hamilton-Jacobi equations. *SIAM Journal on Scientific Computing*, 23:707–740, 2001.
- [38] G. M. LIEBERMAN. Regularized distance and its applications. *Pacific Journal of Mathematics*, 117:329–352, 1985.
- [39] G. M. LIEBERMAN. Mixed boundary value problems for elliptic and parabolic differential equation of second order. *Journal of Mathematical Analysis and Applications*, 113:422–440, 1986.
- [40] G. M. LIEBERMAN. Oblique derivative problems in Lipschitz domains. I. Continuous boundary data. *Bolletino Unione Matematica Italiana*, (7) 1-B:1185–1210, 1987.
- [41] G. M. LIEBERMAN. Optimal Hölder regularity for mixed boundary value problems. *Journal of Mathematical Analysis and Applications*, 143:572–586, 1989.
- [42] C. S. MORAWETZ. On the non-existence of continuous transonic flows past profiles. III. *Communications on Pure and Applied Mathematics*, XI:129–144, 1958.
- [43] C. S. MORAWETZ. Potential theory for regular and Mach reflection of a shock at a wedge. *Communications on Pure and Applied Mathematics*, XLVII:593–624, 1994.
- [44] O. A. OLEĬNIK AND E. V. RADKEVIČ. *Second Order Equations with Non-negative Characteristic Form*. American Mathematical Society, Providence, 1973.
- [45] D. SERRE. Écoulements de fluides parfaits en deux variables indépendentes de type espace. Réflexion d’un choc plan par un dièdre compressif. *Archive for Rational Mechanics and Analysis*, 132:15–36, 1995.
- [46] K. SONG. The pressure-gradient system on non-smooth domains. *Communications in Partial Differential Equations*, 28:199–221, 2003.

- [47] E. G. TABAK AND R. R. ROSALES. Focusing of weak shock waves and the von Neumann paradox of oblique shock reflection. *Physics of Fluids A*, 6:1874–1892, 1994.
- [48] A. M. TEDDALL AND J. K. HUNTER. Self-similar solutions for weak shock reflection. *SIAM Journal on Applied Mathematics*, 63:42–61, 2002.
- [49] T. ZHANG AND Y.-X. ZHENG. Conjecture on the structure of solutions of the Riemann problem for two-dimensional gas dynamics systems. *SIAM Journal on Mathematical Analysis*, 21:593–630, 1990.
- [50] Y. ZHENG. Existence of solutions to the transonic pressure-gradient equations of the compressible Euler equations in elliptic regions. *Communications in Partial Differential Equations*, 22:1849–1868, 1997.
- [51] Y. ZHENG. *Systems of Conservation Laws: Two-Dimensional Riemann Problems*. Birkhäuser, Boston, 2001.
- [52] Y. ZHENG. A global solution to a two-dimensional Riemann problem involving shocks as free boundaries. *Preprint*, 2003.